Chapter 5
Non-Interventional Imaging in Genitourinary Cancer

Shirish G. Prabhudesai, Audrey E.T. Jacques, and Anju Sahdev

Urography

Intravenous Urogram (IVU) (Excretory Urography)

The intravenous urogram (IVU) is a plain film technique, which evaluates the entire renal tract. It consists of a series of plain x-rays of the renal tract followed by intravenous administration of water soluble, iodinated, contrast medium. The injected contrast media is taken up, concentrated and excreted by the kidneys into the ureters and bladder. As the contrast media is radio-opaque, a sequence of plain films taken at precise time points allows assessment of different parts of the renal tract. The contrast medium is excreted by the kidneys enabling visualisation of high-density contrast filled calyces, renal pelvis, ureters and bladder. Tumours, calculi and blood clots are demonstrated as filling defects (Figs. 5.1 and 5.2). The IVU forms part of the initial workup for patients with unexplained renal angle pain, suspected renal calculi, haematuria, renal obstruction and suspected congenital (inherited) abnormalities. With recent advances in CT and MRI technology, the future of the IVU is a subject of ongoing debate [1], although at present it still remains integral to the diagnosis and surveillance of urothelial malignancy.

S.G. Prabhudesai, MBBS, MS, MRCS (✉)
Department of Radiology, St Bartholomew's and
The Royal London Hospital, London, UK
e-mail: shirish.prabhudesai@bartsandthelondonnhs.uk

A.E.T. Jacques, MDDS, BSc, MRCP, FRCR
Department of Radiology, Guy's and St. Thomas Hospital, London, UK

A. Sahdev, MBBS, MRCP, FRCR
Department of Imaging King George V Block, St. Bartholomew's Hospital,
London, UK

V.H. Nargund et al. (eds.), *Urological Oncology*,
DOI 10.1007/978-0-85729-482-1_5

Fig. 5.1 IVU plain films showing stones. Plain full length film from an IVU series showing multiple calculi in the lower pole calyces of the left kidney. Calculi are best demonstrated prior to injection of intravenous contrast media, as the high density contrast can obscure small calculi

In an emergency setting, low dose unenhanced CT through the renal tract (CT KUB) has replaced IVU in patients with painful haematuria and suspected urinary lithiasis. CT IVU has 3 main applications: (1) evaluating the urinary tract in patients with suspected injury. CT IVU is particularly accurate in assessing severity of renal parenchymal and collecting system injury. Injury to the collecting system is seen as contrast extravasation from the intra-renal collecting system, pelvi-ureteric system and urinary bladder (2) confirming the presence of iatrogenic ureteric/bladder injuries following pelvic surgery. This may be seen either as obstruction of the collecting system in instances where the ureter is occluded or as contrast extravasation when the ureter is wholly or partially transected. (3) in patients with unexplained haematuria in the absence of urinary lithiasis-helps in demonstrating urothelial carcinoma that appear as filling defects either in the intra-renal collecting system, ureters or the urinary bladder.

Fig. 5.2 IVU small subtle upper tract TCC lesion. Full length film from an IVU series demonstrating a large filling defect in the bladder, confirmed as a large TCC on cystoscopy (*black arrows*). Within the lower pole calyces there are small subtle filling defects (*white arrows*) which were suspected further foci of TCC. This was confirmed on the cystonephroureterectomy specimen

Patient Preparation for IVU and CT IVU

The patient is starved for at least 4 h prior to the study and is ambulant for 2 h, in order to reduce the amount of bowel gas overlying and obscuring the renal tract. The routine use of purgatives is no longer employed as it does not significantly improve diagnostic quality. Fluid restriction is no longer advocated as dehydration is associated with an increased risk of contrast medium nephrotoxicity. The patient is advised to empty their bladder prior to the examination. Diabetic patients on Metformin no longer need to stop medication but require close monitoring if their blood sugar either by the patient or general practitioner. Pregnant women are advised not to undergo an IVU unless potential benefits outweigh risks to the fetus.

Table 5.1 Cautious use of iodinated intravenous contrast medium (ICM)

1. History of previous allergic reaction to ICM: absolute contraindication to use of ICM excluding those with previous mild flushing or nausea
2. Asthmatics: prophylactic oral steroid cover given prior to the procedure according to local policy and guidelines
3. Those at risk of nephrotoxicity;
Renal impairment (can be given to patients with renal failure having regular dialysis when discussed with clinical team)
Known diabetic nephropathy and those on Metformin (follow local guidelines regarding the use of ICM in patients on Metformin)
Severely debilitated and dehydrated patients

Precautions and Contraindications

Patients with diabetes, multiple myeloma, sickle cell disease and infants are at increased risk of nephrotoxicity and good hydration prior to the examination is advised in these patients. Renal impairment is a relative contraindication for the use of iodinated contrast medium due the risk of precipitating severe renal failure. Poor renal function results in poor renal contrast uptake, concentration and excretion, thereby limiting visualisation of the collecting system. Those with mild renal impairment may be given iso-osmolar non-ionic iodinated contrast medium such as Iodixanol, which is less nephrotoxic than standard non-ionic iodinated contrast agents in this group [2]. Patients with a history of previous severe contrast medium reaction should be excluded (Table 5.1).

IVU Technique

An initial full-length film to include the renal area and bladder is taken to assess technical factors and identify renal calcification, which may become obscured on later contrast enhanced films. A standard adult dose of 50 ml of 350–370 g Iodine/ml (I/ml) or 100 ml of 300gI/ml contrast medium is administered intravenously. This can be altered for patients larger or smaller than the average sized 70 kg adult. A standard sequence of films is obtained at timed intervals, with variations tailored to the individual. The series includes; immediate, 5 and 10-min post contrast renal area films, 15-min full length and post-micturition films. The immediate post contrast film demonstrates renal parenchymal enhancement with contrast medium uptake in the proximal tubules and is termed the nephrographic phase. This enables renal size, position, contour and parenchymal integrity to be evaluated. Excretion of contrast medium into the calyceal system is seen from the 5-min film onwards. Collecting system opacification can be augmented with the use of abdominal compression and a variety of devices are available for this. Compression serves to impede ureteric emptying and enhance pelvicalyceal distension and is applied after the 5-min film if the pelvi-calyceal system is not obstructed. Compression is

contraindicated in patients with acute abdominal pain, recent surgery, a known abdominal aortic aneurysm or other large abdominal mass. Compression is released once adequate views of the upper tract have been achieved. This is followed by full-length film to demonstrate contrast medium within the lower ureters.

Diagnostic Value of the IVU

Deformity or calyceal compression or distortion of the renal contour seen on nephrographic phase images indicates a focal parenchymal mass. The nature of the focal mass cannot usually be determined further on IVU and the differential diagnosis includes a simple cyst, renal carcinoma or other benign lesions. In practice, ultrasound or CT are indicated for detection and characterisation of focal renal masses. In the investigation of haematuria, IVU images must be carefully examined for presence of any filling defect within the renal collecting system, ureters or bladder, which may indicate urothelial tumours. These are frequently small and may be seen as a broad based flat or polypoid filling defect arising from the wall. In some cases, slight irregularity of the wall may be the only indication of a tumour (Fig. 5.2). Large tumours may cause obstruction and dilatation of a single or group of calyces (Fig. 5.3). As urothelial carcinomas (UCa) arise on a background of dysplastic urothelium, bilateral or multiple synchronous or metachronous lesions may occur in up to 38 % [3, 4]. The IVU still has a role in excluding multifocal disease in patients with bladder cancer, and in the follow up and surveillance of treated patients.

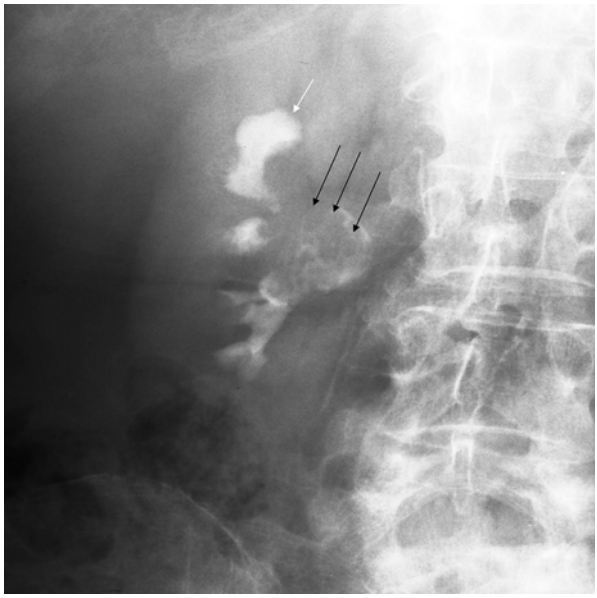

Fig. 5.3 IVU Large lesion with dilated and amputated calyx. A cross-renal image demonstrating a large renal pelvic TCC (*black arrows*). The lesion invades and obstructs the infundibulum of the upper pole calyx resulting in a dilated, obstructed and amputated upper pole calyx (*white arrow*)

Alternatives to the IVU

Multi-detector row CT (MDCT) has made a significant impact in all areas of radiology in recent years (see "Computed tomography" section). It enables the fast scanning of a large volume of the patient in a single breath-hold. Thin slices as narrow as 1.25 mm, of the patient can be reconstructed resulting in much improved spatial resolution. These images can be further reconstructed into sagittal and coronal planes. Images of contrast filled structures can be also reconstructed to produce CT angiographic images in 3 dimensional planes. CT has almost entirely replaced the IVU. Plain non-contrast CT KUB has replaced the IVU in the diagnosis and management of stone disease. In the work up of haematuria, when renal tract malignancy is suspected, CT IVU has an increasingly important role. Excretory phase CT can now be used to evaluate the calyces, renal pelvis and ureters and provide images akin to that of a standard IVU [5] (Fig. 5.4).

CT urography is performed with a combination of unenhanced, nephrographic phase and excretory phase imaging. As in standard IVUs, renal tract calcification is detected on unenhanced images and focal renal parenchymal lesions are detected

Fig. 5.4 Normal CT IVU. (**a**) A maximum intensity projection image from a CT IVU series demonstrating normal renal calyces, ureters and bladder. Peristalysis within both ureters can result in under distension, as seen in the distal right ureter or as linear areas of contrast interruption as seen in the left ureter (*arrows*). (**b**) Volume rendered 3D image from the same patient demonstrating the detail of the renal parenchyma overlying the calyces the whole length of the ureters and bladder

Fig. 5.4 (continued)

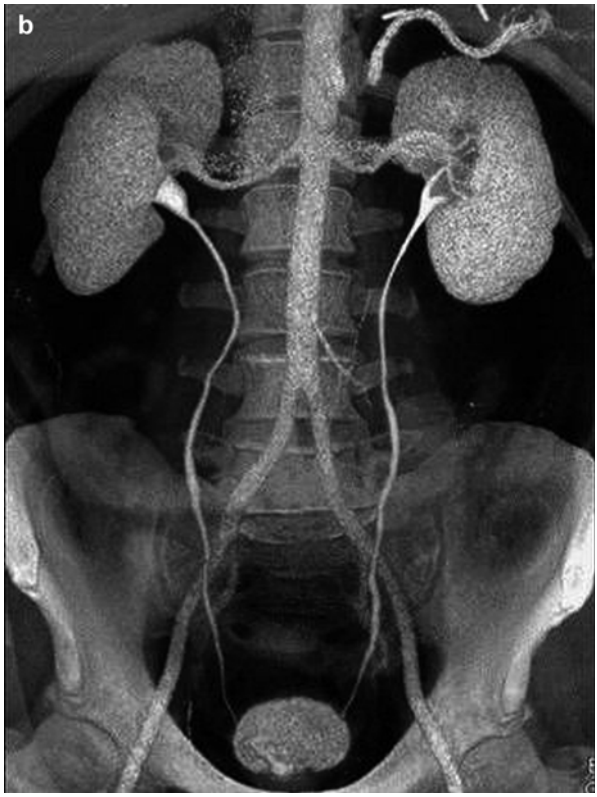

and characterised on corticomedullary (40-s) or nephrographic phase (90-s) imaging. Images obtained 10–15 min after intravenous contrast administration demonstrate contrast filled calyces, ureters and bladder (excretory phase) and are ideal for evaluating the urothelium and filling defects within the collecting systems. The advantage of this technique is that comprehensive evaluation of the renal tract can now be achieved during a single examination [6, 7]. The disadvantages of the technique include cost and time implications as well as radiation dose considerations. The estimated dose equivalent for the CT urogram is approximately 14.8 mSv +/– 3.1 (standard deviation) compared with about 1.5 mSv for a typical standard IVU [8]. However, recent studies using dual phase split bolus protocols, which obtain images in the nephrogenic and delayed phases simultaneously have shown approximately 65 % reduction in radiation exposure without associated reduction in the urinary tract opacification [9]. The guidelines published by the European Society of Urogenital Radiology (ESUR) in 2008 justified the use of CT urography as the first-line imaging investigation for patients with macroscopic haematuria at high-risk for urothelial cancers. They defined high risk as patients above 40 years, macroscopic haematuria, smoking history, history of current or previous GU malignancy and occupational exposure to urothelial carcinogens [10].

Magnetic Resonance (MR) Urography

MR Urography combines the advantage of CT urography in being able to investigate both the renal parenchyma and the urothelium in a single examination. MRI is safe for patients with iodinated contrast allergies or radiation exposure considerations where standard IVU or CT urography are contraindicated e.g. pregnancy. Both dilated and non-dilated renal collecting systems can be visualised using MR urography which is achieved by using either heavily T2-weighted (T2W) sequences or gadolinium-enhanced T1 weighted (T1W) sequences [11]. Heavily T2W MRI sequences generate high signal intensity from simple fluids such as urine, while suppressing signal intensity from surrounding tissues.

Thin section coronal images of the urine filled collecting system provide IVU like images. T2- weighted techniques are fast imaging techniques, which can be successfully applied to patients presenting with painful hydronephrosis of pregnancy in the detection of calculi. In this group of patients both standard and CT IVUs are contraindicated due to the radiation burden and necessary use of iodinated contrast media (Fig. 5.5). Gadolinium-enhanced MR urography relies on

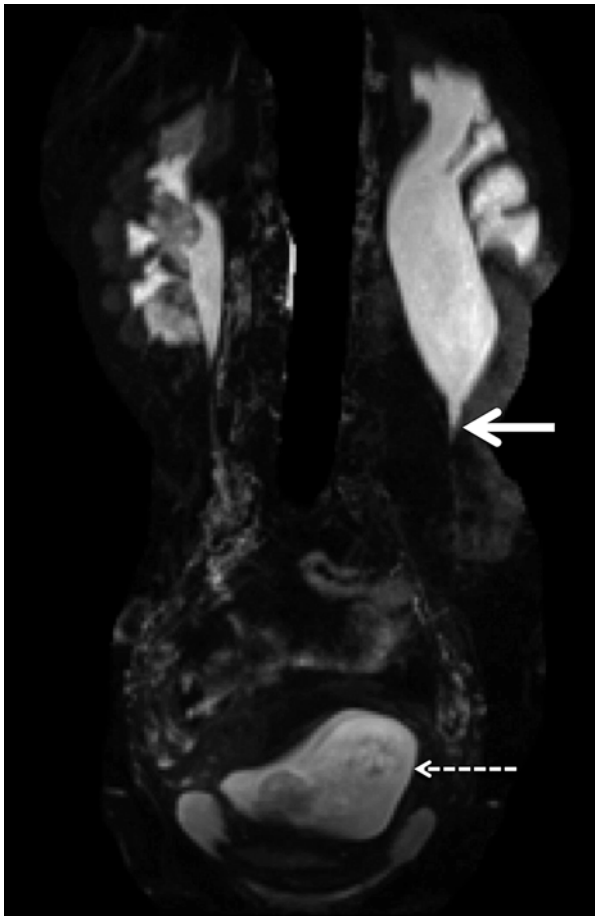

Fig. 5.5 Magnetic resonance urography. Coronal MRU in a pregnant woman presenting with left loin pain and hydronephrosis. The *solid arrow* demonstrates a typical PUJ obstruction as the cause of the hydronephrosis. The *dashed arrow* shows the early gravid uterus

contrast excretion in the same way as standard or CT urography to visualise the collecting system. Suboptimal collecting system opacification may limit this technique in the presence of markedly impaired renal function or high-grade urinary obstruction. While the presence and level of ureteric obstruction can be evaluated, the absence of signal from calculi makes them difficult to visualise with both MRI techniques.

Ultrasound

General Principles

Ultrasound imaging is based on the principle that when sound waves are directed into the body by a transducer placed on the skin surface, some will be reflected back to the body surface and detected by the same transducer. The transducer surface is made of material that has the unique property of expanding or contracting when a voltage is applied across it, known as the **piezoelectric effect**. When the transducer is in contact with skin and a voltage applied, the piezoelectric material expands and compresses an adjacent layer. This pressure induces a corresponding voltage to the next layer of the material, which also expands. The mechanical energy thus created by this wave of compression within the probe is transmitted to the skin surface and propagates through the patient. The propagation and reflection of sound wave through the patient is dependent on density and elasticity of the tissues (**acoustic impedance**). Reflected echoes returning from the patient to the probe induce a voltage which can be detected by the transducer and converted into a **grey scale image**. The reflection of sound waves is greatest where there is a large difference in acoustic impedance of two tissues. Thus soft tissue structures reflect more echoes than fluid and appear bright or echogenic. Fluid, which absorbs sound, appears dark, or **hypoechoic**. The time delay between the initiated and returning pulse to the probe is proportional to the distance the beam has travelled, and spatial information as to the position and depth of tissues are incorporated into the image composition. Constant pulses of sound waves are produced to generate fast real time images of moving body tissues, including flowing blood (**Doppler ultrasound**). Bone and air reflect sound and cannot be imaged, whereas fluid in simple cysts or bladder does not reflect sound waves, which pass through and are available for imaging deeper structures, a phenomenon termed acoustic enhancement. This is of use in the pelvis where the urine filled bladder is used as an acoustic window for visualising deeper pelvic organs such as the prostate gland and uterus.

Advantages

Ultrasound (US) is a non-invasive real time imaging method, does not use ionising radiation, and is well tolerated by patients. The examination does not require special preparation. It poses no real risk to patients making it ideal for repeated surveillance imaging without the radiation burden associated with CT.

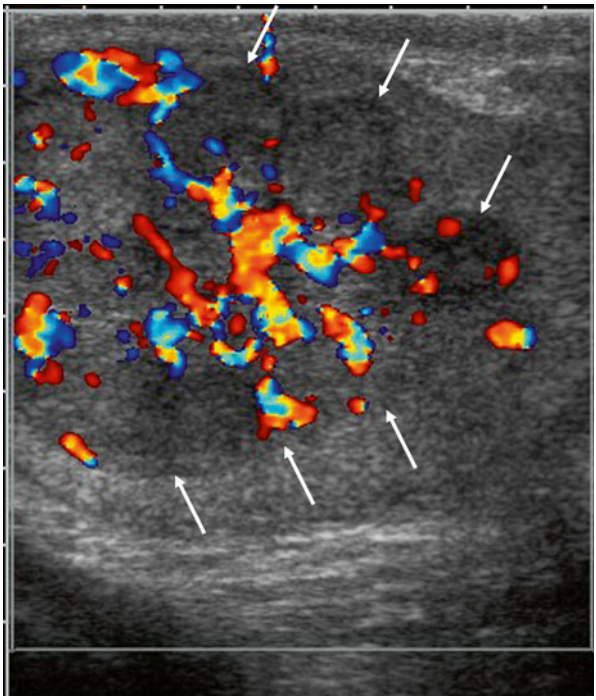

Fig. 5.6 Testicular non seminomatous germ cell tumour. Ultrasound image of a large heterogenous testicular mass (*white arrows*) replacing the whole testes with increased vascularity. Although the ultrasound features are non-specific, the combination of a focal mass and increased vascularity is high suggestive of a germ cell tumour

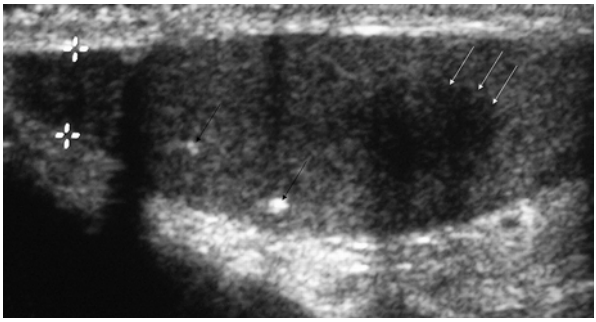

Fig. 5.7 Testicular seminoma. Ultrasound image demonstrating a small focal testicular lesion (*white arrow*) on a background of testicular microlithiasis (*black arrows*). The lesion is poorly vascular and well defined. The lesion was confirmed as a testicular seminoma

The ability to image flowing blood in real time is a major advantage of ultrasound, which can detect tumour extension into the renal vein and IVC in the case of renal and adrenal carcinomas. The demonstration of vascularity within a lesion can aid its characterisation (Figs. 5.6 and 5.7). The real time aspect of ultrasound is well suited to guide procedures such as fine needle aspiration, biopsy and drain insertions. The echogenic tip of a biopsy needle for example, can be easily demonstrated with ultrasound, providing a clearly visible route for safe insertion. Intraoperative ultrasound probes have also been designed which can be used to localise tumours during a radiofrequency ablation and partial nephrectomy.

Disadvantages

The success of US is very **operator-dependent** and images may not always be reproducible between different operators. Although a representative sample of reference images are usually saved onto hardcopy or digital archiving, images are generally best appreciated dynamically during the scan. Comparing a current study with saved hardcopy images from a previous study is not as accurate as it is with CT or MRI.

Patient factors such as body habitus may influence the quality of the images produced with greater attenuation of the ultrasound beam occurring in larger patients, resulting in poor visualisation of deeper structures. As the ultrasound beam is absorbed by air, the presence of prominent bowel gas in the abdomen or pelvis may limit visualisation of deeper organs.

Ultrasound in Genito-Urinary Cancers

There is a wide application of US in genitourinary cancers. Some of these indications are summarised in Table 5.2

Table 5.2 Role of ultrasound in urologic oncology

A. Kidney
1. Investigation of haematuria
2. Detection of incidental renal cell carcinoma
3. Characterisation of cystic renal lesions
4. Distinguish between adrenal and upper pole renal mass
5. Ultrasound guided intervention: Biopsy of renal masses Radiofrequency ablation of renal cell carcinoma Intra-operative ultrasound to aid nephron-sparing surgery
6. Tumour staging Perinephric and local invasion Venous invasion Characterisation of liver lesions
7. Follow up and surveillance eg. particularly testicular cancer
8. Assessment of suspected hydronephrosis in patients with pelvic malignancy
B. Bladder: Investigation of haematuria
C. Prostate: (Transrectal ultrasound; TRUS): TRUS guided biopsy in patients with raised PSA, TRUS guided insertion of fiducial markers for image guided radiotherapy radiotherapy (IGRT)
D. Testes: Investigation of palpable testicular mass Surveillance of normal testis after cancer treatment Assessment for suitability for partial orchidectomy

Ultrasound of the urinary tract forms part of the early screening of patients with haematuria, aimed at excluding renal cell carcinoma or tumours of the bladder and renal pelvis.

Renal Masses

Renal cell carcinomas (RCC) are typically very vascular solid lesions on US showing multiple collateral vessels or intra-tumoural arteriovenous shunting on Doppler ultrasonography. The widespread use of CT and ultrasound has contributed to the increased detection of incidental renal carcinomas in recent years. Thus more RCCs are being detected at an early, asymptomatic stage which has contributed to improved survival [12, 13]. Ultrasound is used to diagnose and characterise variety of renal lesions. Simple renal cysts are extremely common and when confidently diagnosed on ultrasound need no further follow up unless they become symptomatic. Ultrasound can be used to characterise complex cystic lesions and highlight those which have features suspicious for malignancy and warrant consideration for surgical excision. The features suggestive of malignancy include the presence of thick wall and septae, internal solid components, vascular flow within the lesion and associated retroperitoneal lymphadenopathy. Doppler ultrasound is highly sensitive for the detection of vascularity, the presence of which in soft tissue components of a cystic mass is suspicious for malignancy. Ultrasound can be used to characterise very small (<1.5 cm) indeterminate renal lesion detected on CT. These masses may represent either solid lesions which will have vascular flow or hyperdense cysts which are hypoechoeic on US and have no internal vascular flow.

The presence of bilateral or multifocal RCCs clearly has an impact on the choice of patient management and careful ultrasound examination of the remainder of the kidney and of the contralateral kidney should be made. This is particularly important in patients with von Hippel Lindau (VHL) syndrome where multiple renal cell carcinomas may exist, often on a background of multicystic kidneys (see Chap. 17). Complex features of any cysts should be carefully evaluated. Renal cell carcinomas arising in small, complex cysts (<1.5 cm) in these patients are typically slow growing and are often followed up for some time.

Ultrasound may be used in conjunction with CT or MRI although ultrasound is less accurate than CT or MRI in RCC staging and perinephric invasion is poorly demonstrated. It is helpful however in diagnosing tumour extension into the renal vein and IVC (Fig. 5.8) which can be diagnosed with up to 75 % sensitivity [14], or higher when clinically important IVC thrombus is considered [15]. Supradiaphragmatic extension is not well seen and if suspected, echocardiography should help to exclude tumour extension into the right atrium.

Fig. 5.8 Inferior vena cava thrombus on US. Longitudinal section of the abdominal IVC. The normal IVC is seen as a fluid filled tubular structure (*white arrow*) on ultrasound. A large tumour thrombus is seen as a hyperechoic lesion within the lumen expanding the IVC (*black arrows*). The thrombus is limited to the infra-diaphragmatic IVC with its superior extent clearly demonstrated on US

Urothelial Tumours

Ultrasound is supplemented by IVU in the work up of patients with haematuria. Alternatively for the detection of renal and urothelial lesions, a CT IVU would replace both studies. CT IVU has the added advantage of staging a detected malignancy. The renal pelvis, proximal ureter and bladder can usually be visualised with ultrasound. The ureter however, unless dilated, is not well visualised throughout its length. The bladder should be well filled for its optimal examination with ultrasound as focal areas of wall thickening, representing plaque lesions of urothelial carcinoma can be mimicked by a collapsed bladder wall.

In patients with haematuria, demonstration of an echogenic mass with vascular flow on ultrasound within the renal pelvis, proximal ureter or bladder suggests the presence of malignancy, commonly TCC. Visualisation of the upper tract collecting system is improved in the presence of obstruction where an echogenic mass may be seen outlined by hypoechoic urine. Differentiation of echogenic debris from tumour within the collecting system or bladder can be made by the detection of vascularity within tumours on Doppler scan. Doppler can therefore aid characterise of an extrinsic mass or collecting system filling defect demonstrated on IVU and US. US may demonstrate evidence of extension of tumour outside of the renal collecting system or bladder, but overall staging is achieved with a combination of cystoscopy, CT and MRI.

Adrenal Glands

Normal adult adrenal glands are not usually visualised with ultrasound given their small size and deep location. Incidental adrenal mass lesions may occasionally be detected with ultrasound. Ultrasound may be useful to interrogate a large suprarenal

mass seen on axial CT, to determine its origin, exclude invasion of the liver, kidney, tail of pancreas or IVC and renal vessels. CT and MRI are the investigations of choice for the characterisation of adrenal masses and staging of adrenal carcinoma. Large adrenal masses may be biopsied under US control but only after biochemical exclusion of pheochromocytoma.

Testis

Given its superficial location, the testis is well visualised with ultrasound making it the first line investigation of a patient with a palpable scrotal mass. Benign lesions of the epididymis such as simple cysts are common and when a lesion has been detected clinically, ultrasound is used to determine whether it lies within the testis or not. Benign solid lesions within the testis are extremely rare (dermoids and epidermoids), and all such lesions, in the absence of clinical features to suggest infection, are presumed to be malignant. testicular germ cell tumours are typically solid, heterogeneous masses which may be multiple, and are often highly vascular (Figs. 5.6, 5.9 and 5.10). Careful ultrasound examination of the contralateral testis is essential.

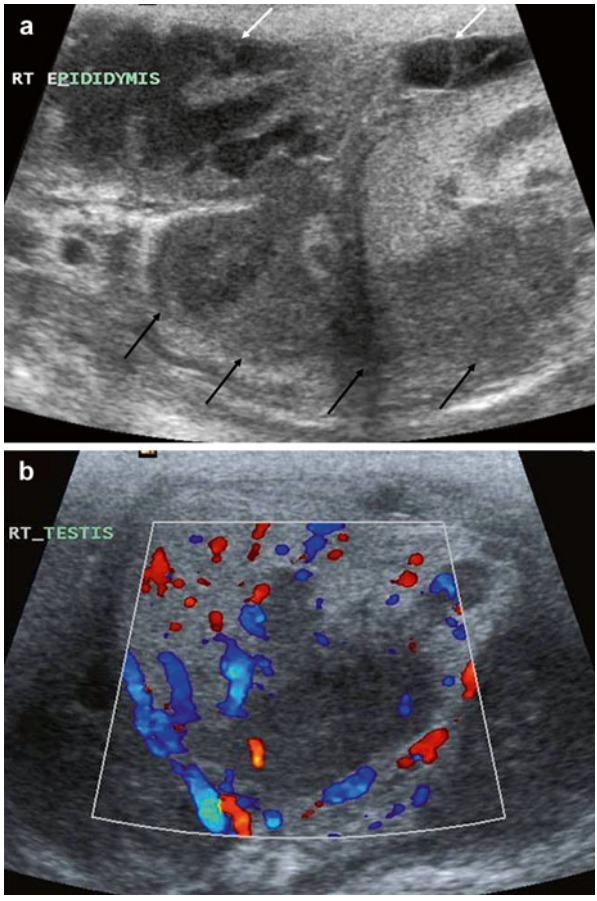

Fig. 5.9 Scrotal TB. (**a**) Longitudinal image of the epididymis which is thickened and hypoechoeic (*black arrows*) with extensive surrounding inflammatory change. There is loculated fibrinous free fluid in the scrotum (*white arrows*) indicating an inflammatory process. (**b**) Transverse image of the testes, demonstrating focal areas of hypoecoic change in the testes with an associated increase in vascularity of the whole testes. These features are highly indicative of an epididimo-orchitis

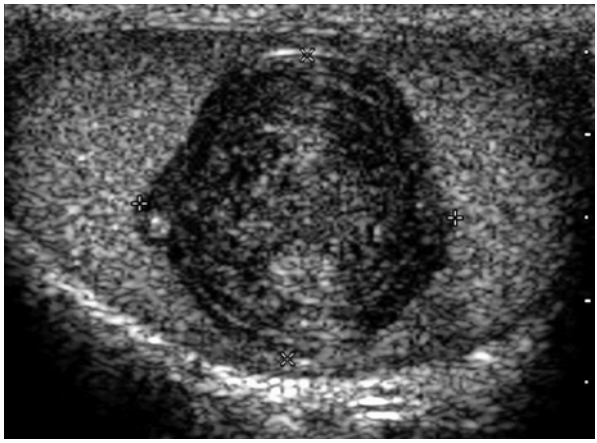

Fig. 5.10 histologically confirmed testicular epidermoid cyst. A longitudinal image of the testes showing a well defined smooth mass with internal laminated rings. These echogenic rings are highly suggestive of an epidermoid cyst

If such a suspicious testicular tumour is detected with ultrasound urgent urology referral should be made. Staging of testicular tumours is primarily centred on the detection of retroperitoneal lymphadenopathy and excluding distant metastases to the lungs, bone or brain. CT is the imaging modality of choice for staging (see CT staging).

Prostate

Prostate ultrasound is indicated in patients with elevated prostatic specific antigen (PSA) in whom prostate carcinoma is suspected. Locally advanced tumours may be visualised on ultrasound within the bladder, and hydronephrosis due to outflow obstruction by a large or invasive tumour can also be diagnosed.

Endocavity ultrasound with a transrectal transducer (TRUS) places the beam in close proximity to the prostate gland. This is performed with the empty bladder. Anatomical detail of the prostate gland can be appreciated with clear delineation between the central and peripheral zones. Tumours are demonstrated as well defined hypoechoic nodules within the peripheral zone with increased vascularity on colour flow Doppler (Fig. 5.11). Carcinomas may also be ill defined and isoechoic or hyperechoeic to the normal prostate gland. Carcinomas in the central gland cannot be distinguished from benign adenomatous changes of the central zone. Ultrasound guided targeted and non-targeted biopsy of multiple sites of the peripheral zone is the main indication for TRUS, in those suspected of prostate carcinoma. Local staging is best achieved with MRI in those considered for radical treatment and with CT for advanced carcinomas to identify nodal disease and distant metastases. This is described in detail later..

Contrast Enhanced Ultrasound

In recent years intravascular contrast agents have been developed which when administered enhance both grey scale and Doppler ultrasound [16, 17]. The ultrasound contrast agents, which have been developed consist of small (<7 μm),

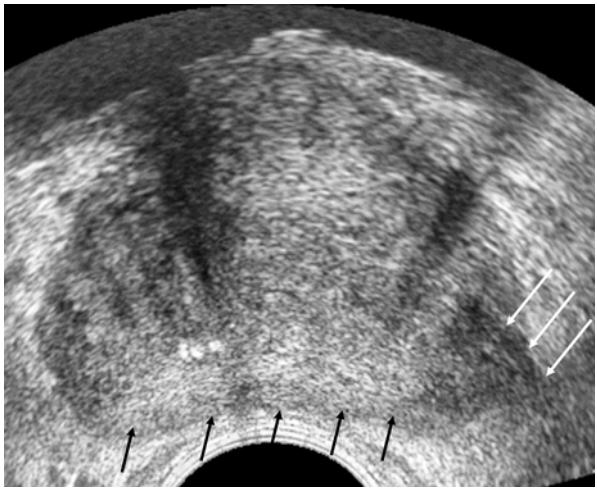

Fig. 5.11 Transrectal ultrasound of the prostate. Transverse section through the mid gland of the prostate. The peripheral gland is seen a homogenous hyperechoic area (*black arrows*). A focal carcinoma is noted within the left peripheral zone as a hypoechoeic area (*white arrows*). This extends beyond the prostatic margins into the peri-prostatic fat indicating extra-capsular disease

encapsulated microbubbles. They are small enough to pass through the pulmonary and capillary circulation and stable enough to withstand hydrostatic pressure within the vascular system and acoustic pressure from the ultrasound wave. When administered they remain in the vascular system. Specific properties of the microbubble capsule and gas within induce greater reflection of the acoustic wave, resulting in increased backscatter. This increases the echogenicity and enhances the grey scale or Doppler image. New ultrasound imaging parameters have been developed which increase the conspicuity of microbubble enhanced backscatter.

The images produced using US contrast agents are greatly enhanced compared to standard grey scale and Doppler imaging and may aid in the detection and characterisation of small isoechoic renal or prostatic malignacies.

Computed Tomography

General Principles

The production of an image by Computed Tomography (CT) is based on differential absorption of an x-ray beam by tissues within the body in the same way as conventional radiography. The amount of absorbed x-rays depends on tissue density, with dense tissue absorbing greater number of x-rays and thereby appearing whiter than less dense tissue which absorb fewer x-rays.

In CT the x-ray beam is collimated into a narrow beam, which passes through a thin slice of the patient. The attenuated x-ray beam, emerging from the patient, is absorbed by detectors, which are capable of differentiating very subtle differences in tissue density. CT therefore has a much greater contrast resolution than plain x-rays and eliminates problems of superimposition of overlying structures to

a much greater extent. The information collected by the detectors is converted into an arbitrary scale (Hounsfield units; HU) based on the attenuation of the x-ray beam by the tissues it has passed through, which varies with differing densities of body tissues. Bone or calcification are the most attenuating and are given a value of +1000HU while air, the least attenuating is given a value of −1000HU. The values are converted to a grey scale image and assigned a brightness level with the highest numbers white and the lowest numbers black. The range (window width) and mean value (window level) of density units is selected to optimise visualisation of different tissue densities of interest. Tissues of densities outside of the range selected will not be discernable and be either totally black or totally white. Standard settings can be selected to display lung, bone or soft tissue 'windows' as required.

Types of CT

Spiral CT

Newer generation scanners utilise a method of volume rather than slice by slice acquisition. A continuous fan x-ray beam, rotating around the patient, traces a spiral path as the patient is moved through the gantry of the machine. Data is continuously acquired through each 360° rotation. Thus a volume of tissue per rotation rather than a slice is imaged. The distance the patient is moved through one revolution of the tube is equal to the slice thickness. Decreased scan acquisition time is a significant advantage of this technique enabling imaging of a larger volume of the patient in a singe breath-hold. This eliminates problems with variation of respiration with each slice. Partial volume effects are also minimized.

Multi-detector CT (MDCT)

It is now possible to acquire data from more than slice thickness simultaneously using parallel banks of detectors. Spiral scanners are now available which are able to acquire up to 128 slice thicknesses in one tube rotation. Data is thus acquired much faster than with a single slice or spiral scanner.

Much thinner slices can be acquired resulting in greatly improved spatial resolution and reduced partial volume effects. In addition, post processing of the large volume of thin slices acquired enables 3 dimensional (3D) and multiplanar image reconstruction. 3D reconstruction applications include CT angiography, virtual endoscopy and CT 'fluoroscopy'. Multiplanar images enable the tumour and its relationship to surrounding structures to be delineated accurately. Combined with CT renal angiography it plays an important role in preoperative surgical planning for renal cell carcinoma, particularly when nephron-sparing surgery is being considered (Fig. 5.12).

Fig. 5.12 3D volume rendered multi-detector CT reconstruction. A coronal 3D reconstruction of the left kidney showing a focal small renal carcinoma (*white arrow*). Its location in the kidney is well demonstrated along with its relation to the central renal vessels. The main renal artery is shown by the *black arrow* and the main renal vein by the *arrow head*. Both have a normal hilar configuration

Patient Preparation and Technique

Oral contrast medium or water is administered prior to the examination to optimise opacification of small and large bowel to allow better anatomical detail, particularly in the pelvis or retroperitoneum, where the presence of unopacified loops of bowel can be misinterpreted as soft tissue masses or lymph nodes. For bladder and prostate tumours a moderately full bladder is preferable.

For characterising space occupying lesions of the kidney or an adrenal gland, initial unenhanced scans are obtained through the renal or adrenal area at 5 mm slice thickness. The scan is obtained in a single breath-hold at either maximum inspiration or expiration. This allows visualisation of calcification within the lesion and enables the density of the lesion to be calculated. The scan is then repeated following administration of intravenous contrast medium unless contraindicated (see Table 5.1). 100 ml of non-ionic iodinated contrast medium (300–350 mg iodine/ml) is administered via a pump injector at a rate of 3–5 ml/ s. To optimise characterisation of liver, renal or adrenal lesions scans are obtained at variable times to maximise vascular enhancement. For renal lesions scans are obtained at 40 s and 90 s following contrast infusion. For adrenal lesions scans are obtained at 60 s and 15 min following contrast administration and for liver lesions, scans are acquired at 30 s, 70 s and delayed scans up to 15 min may be required.

In the kidney 40 and 90 s equate to corticomedullary and nephrographic phases of enhancement respectively. While the nephrographic phase is more sensitive for the detection and characterisation of small renal lesions, evaluation of the kidneys during both phases provides optimum information. Images obtained during the corticomedullary phase detect low grade enhancement in papillary carcinomas and allow for evaluation of the renal vein and identification of accessory renal arteries. Images obtained at 3–15 min post contrast administration demonstrate contrast within the pelvicalyceal system (excretory phase), and can be used to delineate tumour within the renal pelvis or ureter. In centrally located RCCs, the proximity of

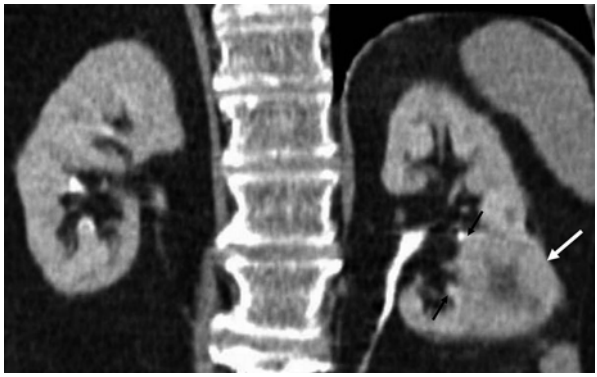

Fig. 5.13 Coronal multi-detector CT reconstruction. A CT IVU coronal reconstructed image. A left lower pole renal cell carcinoma is demonstrated (*white arrow*). The medial margins of the tumour extend up to the renal sinus and abuts the calyces (*black arrows*)

the lesion to the pelvi-calyceal system and the hilar vessels allows evaluation for the suitability for nephron sparing surgery (NSS) (Fig. 5.13).

For a full staging scan, axial 2–5 mm images are acquired through the whole abdomen from the level of the diaphragm to the pelvis. These are obtained with the 90 s scan when a renal protocol scan has been performed. Alternatively, scanning is timed to commence at approximately 60 s following contrast infusion so as to image the liver during maximum portal venous phase enhancement, the optimum time for the detection of most hepatic metastases. For tumours such as renal cell carcinoma and testicular carcinoma which have a propensity to metastases to the lung, images through the thorax are initially acquired at approximately 20–40 s after contrast infusion.

The Role of CT in Urologic Oncology

There are a myriad of uses for CT in urological cancer management. These are summarized in Table 5.3.

Lesion Detection and Diagnosis

CT does not usually form part of the initial diagnosis of bladder, prostate or testicular carcinomas although incidental detection of a soft tissue filling defect within the contrast filled renal collecting system or bladder may suggest the presence of a transitional cell carcinoma. Contrast enhancement of such a mass confirms the diagnosis and excludes the presence of debris or blood clot.

Occasionally testicular carcinoma might present as large retroperitoneal lymph nodal mass and in a young male patient the possibility of testicular germ cell tumour should be considered. CT has an established role in the detection and characterization of indeterminate renal and adrenal lesions.

Table 5.3 Role of CT in Genito-Urinary cancers

A. Kidney
1. Detection of incidental renal cell carcinomas
2. Characterisation of cystic renal mass lesions
3. Tumour staging Local: perinephric and organ invasion Nodal staging Venous invasion Distant metastases: lung, liver, bones, brain
4. 3D CT for surgical planning
5. Follow up and surveillance
B. Adrenal
1. Detection and characterisation of incidental adrenal mass lesions
2. Primary adrenal carcinoma staging: Local and Distant metastases: lungs, liver, bones
3. Planning surgical resection in large adrenal masses
C. Bladder
1. Tumour staging: Locally advanced disease; Nodal: Iliac and para-aortic lymph nodes Distant metastases: lung, brain, liver, bones
2. Radiotherapy planning
3. Post chemotherapy evaluation and surveillance
D. Prostate
1. Tumour staging: Locally advanced disease; Nodal: pelvic side wall and retroperitoneal
2. Rising PSA following radical therapy for nodal or bony metastases
3. Radiotherapy planning
E. Testis
1. Tumour staging, Nodal staging and Distant metastases: lungs, brain, liver and bones
2. Surveillance
3. Planning retroperitoneal lymph node dissection

Renal Space Occupying Lesions

RCCs are suspected on CT in the presence of a wholly or partially solid, enhancing and often heterogeneous parenchymal renal mass, frequently detected incidentally [12, 13, 18]. Cystic renal cell carcinomas are well recognised and need to be differentiated from complicated benign cysts such as simple cysts which have become infected or bled.

Bosniak Grading of Cystic Renal Lesions

A system of grading the appearances of cystic renal masses with CT, according to the presence of features associated with malignancy has been devised by Bosniak [19, 20], is summarized in Table 5.4. Simple cysts with no suspicious features are within **category I** and those with increasingly complex features are graded up to

Table 5.4 Bosniak classification of cystic renal lesions

Category	Description
I	Simple benign cyst with an imperceptible or hairline thin wall that does not contain septa, calcification or solid components. It measures as water density and does not enhance following contrast administration
II	Benign cyst that may contain a few hairline thin septa. Fine calcification may be present in the wall or septa. Uniformly high attenuation lesion of <3 cm that is sharply marginated and does not enhance
IIF	Cyst might contain more hairline thin septa. Minimal enhancement of septa or wall. May be minimal thickening of the wall/septa. Cyst might contain calcification that may be nodular and thick but does not enhance. Does not contain enhancing soft tissue elements. Non enhancing high attenuation lesions >3 cm
III	Indeterminate cystic masses that have thickened irregular wall or septa in which enhancement can be seen.
IV	Cystic lesions are likely malignant that contain enhancing soft tissue elements.

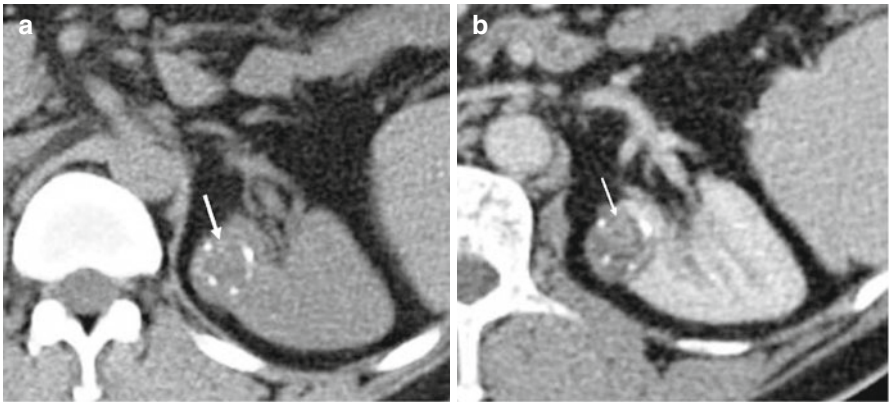

Fig. 5.14 Bosniak 3 renal cyst. (**a**) Pre contrast CT demonstrating a cortical lesion with dense amorphous calcification (*white arrow*). (**b**) Post contrast CT showing small areas of soft tissue enhancement (*white arrow*) within the lesion in keeping with a Bosniak 3 cyst. The lesion was confirmed as a clear cell renal cell carcinoma on histology

category IV, which are frankly malignant. Suspicious features include the presence of thick punctate calcification, wall or septal thickening and the presence of enhancing soft tissue components. **Category III and IV** lesions have malignant features and should be surgically removed (Figs. 5.14 and 5.15). In category III and IV, 60 % of the lesions are malignant and the main benign lesions are inflammatory and infective diseases. **Category II** lesions have some complex features such as fine, linear calcification, thin septa of are of increased density, but no enhancing soft tissue. These lesions do not need to be followed up. More recently category IIF has been introduced and includes benign complicated cysts which require follow up

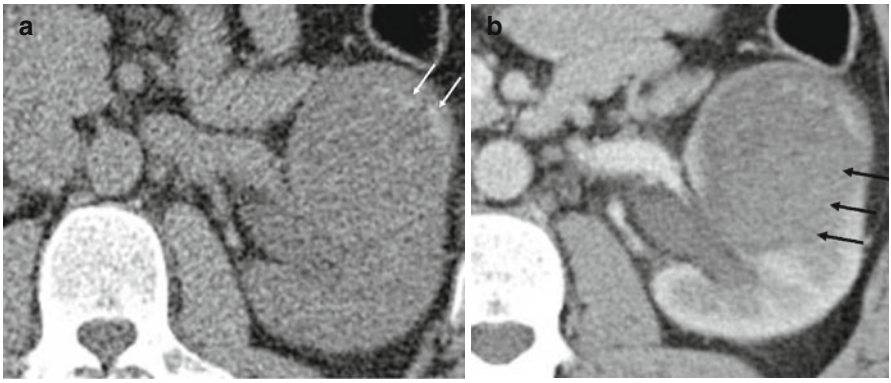

Fig. 5.15 Bosniak 4 renal cyst. (**a**) Pre contrast CT demonstrating a large left renal mass with irregular areas of calcification and low attenuation cystic background (*white arrow*). (**b**) Post contrast CT showing diffuse and homogenous enhancement centrally within the lesion (*arrows*). In view of the size and the enhancement, the lesion is consistent with a Bosniak 4 cyst. The lesion was a papillary carcinoma on histology

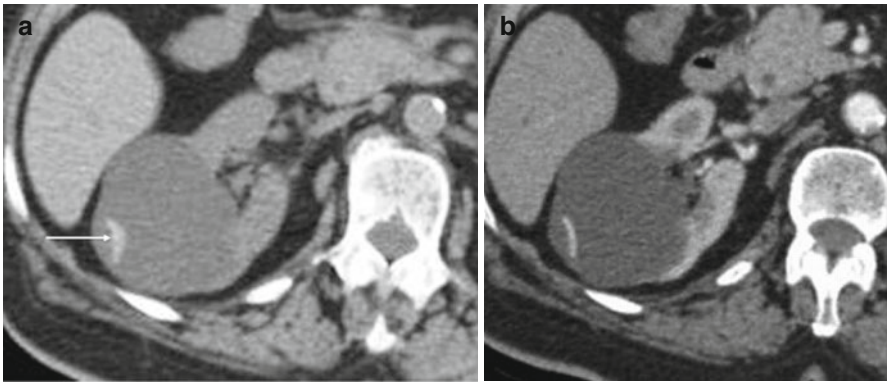

Fig. 5.16 Bosniak 2F renal cyst. (**a**) Pre contrast CT of a large right renal cyst with a focal area of thick calcification (greater than 2 mm) within a septum (*white arrow*). (**b**) Post contrast, no areas of enhancement are demonstrated in the cyst and no other complex features are seen in keeping with a Bosniak type 2F cyst

over time to confirm stability. Features in this group include those with numerous but thin septa, septal or wall enhancement but no soft tissue component, hyperdense category II lesions which are totally intrarenal or greater than 3 cm [21] also fall into this category (Fig. 5.16).

Adrenal Lesions

Adrenal mass lesions are detected incidentally in approximately 4–7 % of the population [22]. They are therefore not an infrequent incidental finding in patients with malignancy. The adrenal glands are also a site of haematogenous metastases from

Fig. 5.17 CT lipid rich adrenal adenoma. Pre contrast CT showing two small homogenous adrenal masses (*black arrows*). Both have low attenuation on CT measuring -6HU and 2HU in keeping with lipid rich benign adenomas

other cancers. In a patient with cancer it is often critical to distinguish between an adenoma and metastases. Adenomas are typically smaller than metastases on unenhanced CT imaging. Metastases are more heterogeneous than adenomas and their margins are not well-defined. However, small metastases may be homogeneous and with well-defined margins. Lesions greater than 4 cm in maximum diameter are suspicious for malignancy, although adrenal metastasis in the absence of a known primary are exceedingly rare [23, 24]. However, 36–71 % of incidental adrenal masses found in known oncology patients are metastases [25–27]. Adrenal cortical carcinomas usually present as very large mass lesions, which may or may not be functioning. Non-functioning carcinomas present later with symptoms related to mass effect. These tumours are usually heterogeneous with areas of enhancement. The differential diagnosis of a large adrenal mass includes adrenal metastasis or phaeochromocytoma. Biochemical correlation will confirm the diagnosis in the latter.

The cornerstone of adrenal imaging is CT, performed before and after intravenous injection of contrast medium and acquired as 3–5 mm scans through the adrenal glands. Most adenomas contain an abundance of intracellular lipid and have relatively low density on unenhanced scans. An inverse relationship between percentage fat content and attenuation value on unenhanced CT has been shown [28], with lipid rich adenomas characterized by density measurement of 10HU or less (Fig. 5.17). When a pre-contrast upper threshold measurement of 10HU is taken for a homogenous adrenal mass, a sensitivity of 71 and 98 % specificity is obtained in the diagnosis of a benign adenoma [29]. However, a subset of adenomas cannot be diagnosed on the basis of their unenhanced CT attenuation as they lack intracellular fat. The diagnosis of both lipid poor and lipid rich adrenal adenomas can be made with a high degree of certainty on CT based on their contrast medium enhancement

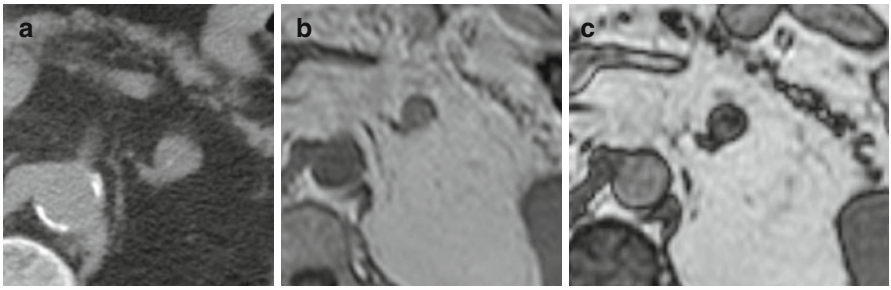

Fig. 5.18 CT and chemical shift MRI of a lipid poor adrenal adenoma. (**a**) Pre contrast CT showing a small homogenous left adrenal mass with a CT attenuation value of 20HU. An attenuation value greater than 10HU indicates an indeterminate mass. (**b**) In phase MRI of the adrenal mass. (**c**) Out-of-phase MRI showing loss of signal intensity in the adrenal mass, in keeping with a benign adenoma

washout patterns [30, 31]. Adenomas typically enhance early with rapid contrast medium washout, compared with non-adenomas which washout over a longer time period. By taking attenuation value measurements of the adrenal lesion at 0 s (unenhanced), 60 s (initial enhancement) and 15 min (delayed enhancement) following contrast medium administration, the absolute and relative percentage contrast washout can be calculated as follows;

$$\text{absolute percentage washout} = \left(\text{initial} - \text{delayed} / \text{initial} - \text{unenhanced}\right) \text{x}\, 100$$

$$\text{relative washout} = \left(\text{initial} - \text{delayed} / \text{initial}\right) \text{x}\, 100.$$

Absolute percentage washout of >60 % and relative percentage washout >40 % are used to make a diagnosis of adrenal adenoma with sensitivity and specificity of 88 % and 96 % and 96 % and 100 % respectively [30, 31]. Chemical shift sequences on MRI are used to characterize atypical, lipid poor adenomas which remain indeterminate by contrast medium washout criteria on CT (Fig. 5.18), or if CT and iodine based contrast media is contraindicated.

New guidelines published by the American College of Radiology Incidentally detected Abdominal and Pelvic Lesions Committee, suggest that for lesions >4 cm in size which do not have typical imaging features seen in myelolipomas, adenomas, cysts etc., adrenal resection should be considered after biochemical evaluation to exclude phaeochromocytomas, without any other additional imaging workup [32]

Tumour Staging by CT

Tumour staging is vital to predict prognosis and for planning the treatment strategy. Staging of the primary tumour with reference to its size, evidence of invasion of local structures, nodal involvement and distant metastases forms the basis of

the internationally accepted TNM classification system. While not specifically a radiological classification system, CT is well placed to demonstrate these features well. However, the sensitivity and specificity of the accuracy of CT varies with tumour type and location.

Local Assessment of the Primary Tumour

CT is well suited to assess certain urologic tumours, in particular, renal cell carcinoma, adrenal and large bladder cancers. Superficial bladder tumours not invading the muscle layer, localised prostate carcinomas, and testicular tumours are best assessed with cystoscopy, MRI or ultrasound respectively. Local tumour invasion is diagnosed on CT where tumour is seen extending into surrounding fat or adjacent organs. Loss of the fat plane between tumour and adjacent structures is not always a reliable indicator of invasion. This is particularly the case in the pelvis where clear fat planes are not normally visible on CT between the posterior bladder wall, prostate, cervix, uterus and rectum. Locally advanced bladder or prostate carcinoma is best diagnosed on MRI when enhancing soft tissue is seen directly invading adjacent structures. Other clues may be present which raise the suspicion of local tumour extension. For example, tumour involvement of the ureteric orifices in the bladder may be suspected in the presence of hydronephrosis. The good contrast resolution of CT enables visualisation of abnormally placed pockets of gas, in the bladder or vagina for example, which may raise the suspicion of vesicovaginal or colovesical fistulae secondary to tumour invasion.

Lymph Nodes

The detection of tumour extension to lymph nodes by CT is dependent on an assessment of lymph node size. A short axis diameter of above 1 cm is considered abnormal in the upper retroperitoneum, and above 8 mm within the pelvis.

These measurements are however somewhat arbitrary and normal or reactive nodes may frequently be larger. The limitations of using size criteria have been evaluated in renal cell carcinoma where nodes greater than 1 cm contain normal or hyperplastic lymphoid tissue in up to 43 % of cases [33, 34]. The presence of enlarged reactive local nodes is increased further in the presence of tumour necrosis and venous invasion [35]. Similarly, micrometastases within normal sized lymph nodes accounts for false negative rates of up to 4 % in one series [35]. Other features to suggest lymph node involvement include, round rather than oval shape, irregular contour, attenuation and contrast enhancement similar to the primary tumour, and necrosis.

Knowledge of the lymphatic drainage pathways of different tumour is essential in the CT evaluation for lymphadenopathy and particular attention should be paid to the retroperitneum in the case of testicular carcinoma and the pelvic side walls in the case of bladder and prostate carcinomas.

Distant Metastases

Unlike ultrasound and MRI, CT has the advantage of being able to image a large volume of the patient in a single scan. It is therefore the ideal imaging modality to detect distant metastases.

Scans of the thorax and liver are included as part of the standard staging for renal, adrenal and testicular malignancies and scan technique is optimized to demonstrate lesions in different sites, as discussed above. Bone metastasis will be diagnosed on CT if present in the areas covered in the scan and when the images are viewed on settings optimised for visualising bone ('bone windows'). They may be visible as sclerotic or lucent defects in the bone, which may or may not expand the bone contour. Attention should be paid to the bones, particularly vertebrae, in patients with renal cell, testicular and prostate carcinomas. Renal and testicular cancer metastases are classically lytic lesions whilst prostatic metastasis are sclerotic lesions. CT of the brain following intravenous injection of contrast medium may be performed acutely in patients presenting with neurological signs to exclude brain metastases, particularly those with testicular germ cell and renal cell carcinomas. In this group, MRI is more sensitive but is reserved for those with clinical suspicion and a negative CT and is only performed routinely in those patients considered at high risk of developing brain metastases.

Tumour Staging: Disease Specific Considerations

Renal Cell Carcinoma

The widespread use of cross sectional imaging has resulted in the detection of earlier stage renal cell carcinomas. Accurate preoperative staging is essential to plan an appropriate management strategy. The differentiation between tumours limited to the kidney (T1-2) and tumours with perinephric invasion (T3) can be difficult on imaging although it is not clinically significant in patients treated with radical nephrectomy. However, since the introduction of nephron- sparing surgery and radiofrequency ablation for low stage tumours it is now essential that this distinction is made preoperatively. The most reliable indicator is the presence of focal soft tissue within the perinephric fat, measuring up to 1 cm being 98 % specific for diagnosing stage IIIa disease. However this sign is not often seen [36]. The presence of soft tissue stranding extending into the perinephric fat is suggestive of tumour invasion, or it can also be due to tumour induced fibrosis, oedema and inflammation. This finding is present in up to 50 % of those with stage I tumour confined to the kidney [36]. Gerota's fascia is well visualised on CT in most patients and tumour extension beyond is diagnostic of stage 4 disease (Figs. 5.19 and 5.20).

The presence of tumour invasion into the renal vein occurs in up to 25 % of patients with renal cell carcinoma and into the IVC in up to 10 % [37, 38]. Estimation

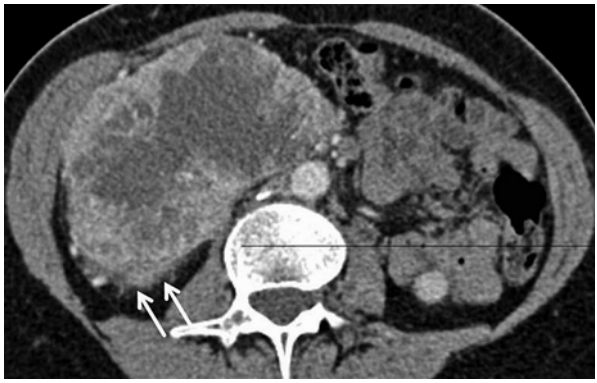

Fig. 5.19 RCC with peripnephric changes. Post contrast enhanced CT of a large right sided renal carcinoma. Along the posterior margin, tumour stranding is seen in the perinephric fat (*arrows*) in keeping with a T3a carcinoma

Fig. 5.20 RCC invading the psoas. Large right renal cell carcinoma arising from the lower pole, invading the right psoas muscle (*arrows*) in keeping with a T4 carcinoma

of the upper extent of intracaval tumour is essential for appropriate surgical planning. Indirect signs of IVC invasion include vessel enlargement and the presence of collateral vessels (Fig. 5.21). The most reliable sign is visualization of a persistent filling defect on contrast medium enhanced images (Fig. 5.22). Images must be obtained during peak enhancement of the renal vein and IVC and are acquired at 60 s post intravenous contrast medium administration. CT has been reported to detect intracaval tumour with a sensitivity of 78 % and specificity of 96 % [36] and up to 100 % accuracy has been reported with newer MDCT techniques [38]. Venous invasion is also commonly seen in adrenal carcinomas, with the same implications for surgical planning when there is extension in the IVC. Supra-hepatic caval tumour extension and invasion of the IVC wall can be difficult to distinguish on CT and if suspected an MRI should be performed. A transoesophageal echocardiogram can help to asses the tumour extension into the right atrium.

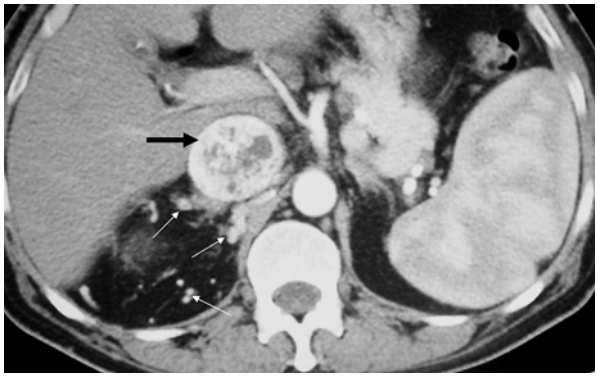

Fig. 5.21 Signs of IVC invasion: IVC expansion. Post contrast CT in a patient with right sided renal carcinoma. The IVC is expanded (*black arrow*) and multiple collaterals are present in the retroperitoneum (*white arrows*)

Fig. 5.22 Signs of IVC invasion: filling defect. Post contrast enhanced CT showing a very large carcinoma in the left kidney. The images are acquired at 90 s after contrast administration, thereby opacifying the IVC. A large filling defect is present in the IVC (*arrows*). The filling defects in this phase within the IVC is consistent with thrombus. Enhancement of thrombus indicates tumour thrombus

Urothelial Cancer

Imaging of the bladder with CT is ideally achieved with a full bladder and intravenous contrast medium. Tumour within the bladder enhances to the same degree or greater than that of normal bladder wall. Tumours may be multifocal and are visualized as either plaque like thickening of the bladder wall or mass like soft tissue protruding into the bladder lumen. The important role of CT in bladder cancer staging is distinguishing between tumour confined to the bladder wall and those which have invaded thorough the wall, into the perivesical fat (stage T3). Full thickness bladder wall invasion is indicated by an irregular outer contour of the tumour and stranding of the adjacent perivesical fat (Fig. 5.23). Invasion into adjacent structures indicates stage T4 disease.

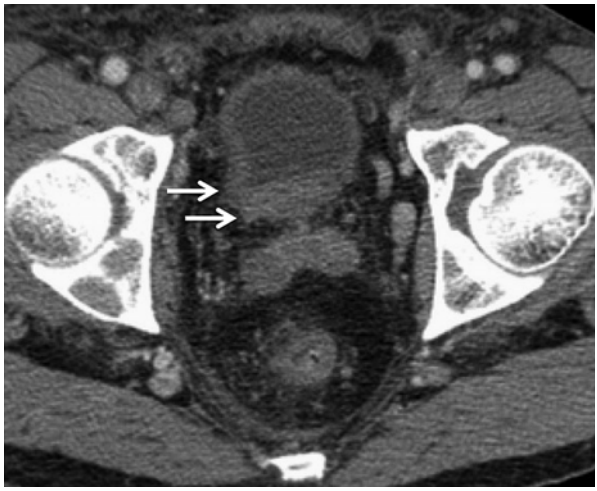

Fig. 5.23 Bladder TCC stage 3a on CT. Large right sided and posterior bladder wall TCC. There is full thickness invasion and stranding (*arrows*) in the peri-vesical fat highly suggestive of tumour invasion

Upper tract TCC can be visualized with CT IVU using the technique described earlier. Focal TCCs may be seen as soft tissue filling defects within a dilated renal pelvis or calyces. Stage T1 and T2 tumours invading the subepithelial connective tissue and muscularis layer respectively cannot be differentiated from each other with CT. Tumour invasion into the renal parenchyma or periureteric fat indicated stage T3 disease and is visualized as areas of poorer enhancement compared to normal renal tissue or nodular projections in the peri-nephric space. (Fig. 5.24).

Tumour invasion through the renal parenchyma and into the perinephric fat indicates stage T4 disease (Fig. 5.25). As with bladder TCC the importance in radiology is in detecting distant and multifocal disease with careful attention made to the contralateral kidney, ureter and bladder.

Testicular Cancer

The role of CT in the management of malignant testicular tumours is to stage the nodal disease accurately and to detect the presence of distant metastases in lungs, liver, bone and brain. Nearly 95 % of testicular tumours are germ cell tumours and these have a predictable pattern of lymphatic spread. Right sided tumours spread to right sided retroperitoneal nodes; pre, para, retro and aortocaval nodes and right renal hilar nodes, while left sided tumours spread to the left retroperitoneum; pre and left para aortic and left renal hilum [39]. The pattern is so consistent that enlarged contralateral nodes in the absence of ipsilateral nodal enlargement are

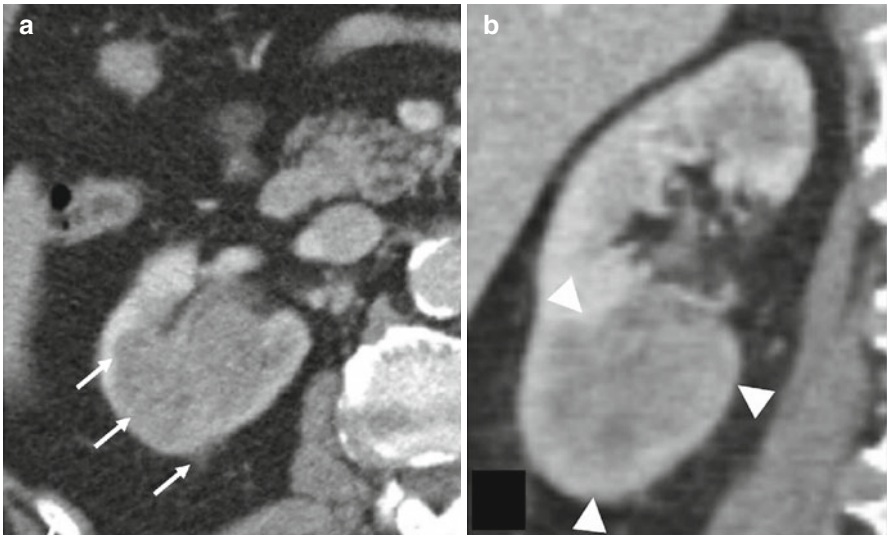

Fig. 5.24 Upper tract transitional cell carcinoma: T3a. (**a**) Axial post contrast CT showing an ill defined diffuse mass replacing the lower pole of the right kidney. The mass is central, replaces the collecting system and invades the renal parenchyma. Small tumour nodules are also seen in the perinephric space in keeping with a T3a transitional cell carcinoma (*arrows*). (**b**) Coronal post contrast reconstructed CT demonstrating the transitional cell carcinoma invades the renal sinus and the full thickness of the renal cortex (*arrowheads*)

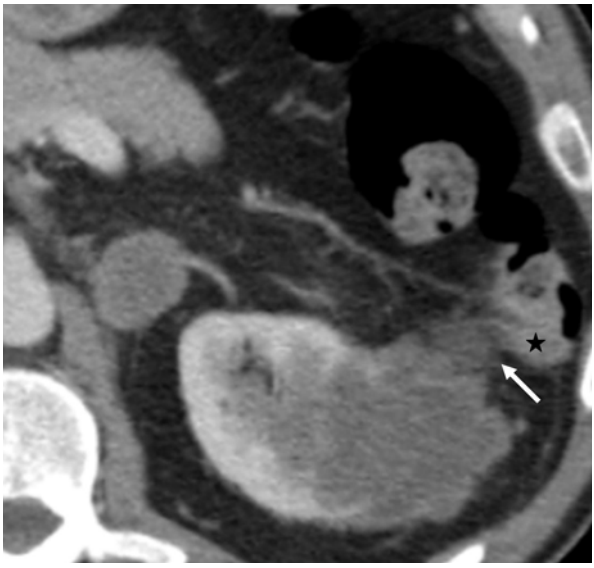

Fig. 5.25 Upper tract transitional cell carcinoma: T4. Axial post contrast image demonstrating a large upper tract transitional cell carcinoma invading the full thickness of the renal parenchyma and extending into the perinephric fat. Direct tumour invasion (*arrows*) is seen into the splenic flexure (*asterisk*) in keeping with a T4 carcinoma

unlikely to be due to tumour. Extension to contralateral nodal groups can be seen in the presence of bulky ipsilateral nodes, greater than 2 cm, and cross over is seen more commonly from right to left sided adenopathy [40]. Extension to lateral nodal

groups anterior to the psoas muscle (echelon nodes) is uncommon but well recognised in testicular carcinoma [41]. Retroperitoneal lymphadenopathy can be mimicked by the presence of unopacified bowel loops or variations in normal vascular anatomy, such as a retro-aortic renal vein or double IVC and can be a potential diagnostic pitfall, particularly if good oral and intravenous contrast enhancement is not achieved. Nodal extension to pelvic nodes is only seen in the presence of massive retroperitoneal lymphadenopathy. Supradiphragmatic extension can occur directly from the retroperitoneum via retrocrual extension and into the posterior mediastinum, or via the thoracic duct to the supraclavicular fossa. These areas should be included in the scan when retroperitoneal lymphadenopathy is present. The lungs are the commonest site of haematogenous disseminated and nodules as small as 3 mm are easily visualised with CT. Disease surveillance however is usually with chest x-ray.

CT Guided Intervention

The good spatial resolution of CT facilitates its use for a variety of image-guided procedures including fine needle aspiration, biopsy and drain insertion. These procedures can usually be performed under local anaesthetic and with minimal distress to the patient.

Technique

Patient positioning on the scan table is critical and should be both optimal for the procedure and comfortable for the patient as it must be maintained throughout the procedure.

A scan through the relevant area is performed initially and oral or intravenous contrast may be used when it is necessary to highlight neighboring vessels or bowel. A reference image is selected from which a direct and safe needle pathway from the skin to the lesion can be identified. Using the guide laser on the CT scanner the selected point can be identified on the patient and marked on the skin. During needle insertion repeated scans through the area can be obtained to establish exact position of the needle tip and ensure correct pathway. CT can be used to guide procedures in areas which are difficult to visualize with ultrasound, particularly the retroperitoneum, chest and deep pelvis.

CT is also used to guide radiofrequency ablation and cryotherapy of renal masses suspected to be RCC. This role is discussed in Chap. 23.

Surgical Planning

Knowledge of the spatial relationships of the tumour to other structures, particularly vessels, is an important consideration for surgical planning. It is important to document the presence of accessory renal arteries or normal variations in the location of

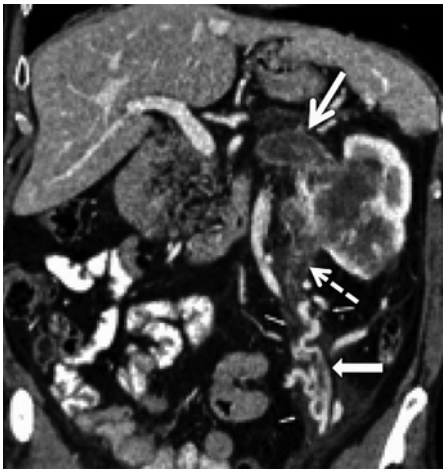

Fig. 5.26 Left sided RCC. Large infiltrative tumour, invading the left renal hilum. The coronal reconstruction demonstrates invasion of the renal vein (*arrow*) and left testicular vein (*dashed arrow*). There is a resultant left sided varicocoele, seen in the abdomen and pelvis (*block arrow*) extending into the scrotum

the renal vein prior to surgery. Multidetector CT (MDCT) enables accurate CT angiographic images of the renal vascular supply to be generated via a variety of techniques. Maximum intensity projection (MIP) images are commonly used to reconstruct angiographic images from pixels with the maximum attenuation value. 3-dimensional (3D) images can be generated which allow the image to be viewed in multiple planes (Figs. 5.12 and 5.26). 3D volume rendered imaging creates a 3D image from the entire data set without preliminary editing and enables the spatial relationship of the tumour to surrounding structures to be displayed. Overlapping structures can be separated out to improve visualisation. 3D volume rendered angiography has been shown to be as accurate as conventional angiography in depicting renal vascularity [42]. 3D images display anatomical detail in a format comparable to surgical appearances compared to conventional axial imaging.

Accurate staging information is essential for the selection of appropriate patients for nephron sparing surgery. It is important to identify patients with bilateral or multifocal tumours, those with stage I disease confined to the kidney, and those without invasion of the collecting system or vascular structures. Lesions most suitable for nephron-sparing surgery are small (usually <4 cm), peripherally located, preferably exophytic, and away from the collecting system and renal hilum. These features are well demonstrated with 3D CT. [43–45].

Imaging in the Post-operative Period

CT is useful in the evaluation of the postoperative patient. A degree of free fluid and inflammatory change will be present in the abdomen or retroperitoneum in the immediate post operative period, along with pockets of gas, particularly following laparoscopic surgery. However, increasing or new intra-abdominal gas and fluid might suggest the presence of anastomotic dehiscence for example following

cystectomy and ileal conduit formation. The detection of an anastomotic leak can be improved with the introduction of 20–50 ml of dilute (2 %) water-soluble contrast medium via the stoma or rectum, where appropriate, prior to CT scanning.

Limitations of visualising deeper portions of the abdomen with ultrasound make CT the more appropriate imaging modality when infected collections are suspected clinically. An abscess can be identified by presence of a focal collection of fluid with an enhancing rim and/or pockets of gas within. Surgeons frequently use oxidized regenerated cellulose (Surgicel) and leave it in the operative bed to achieve intra-operative haemostasis. The immediate post-operative appearance of the inserted Surgicel can mimic that of an abscess and can appear as linear collections of gas within masses of mixed attenuation. Having details of the operative procedure will help differentiate the presence of Surgicel in the operative bed from an abscess [46]. CT can also be used to guide drain insertion into a collection, or plan ultrasound guided or surgical drainage where most appropriate.

Tumour Volume Measurements

The aim of radiotherapy is to maximally irradiate tumour, bladder and prostate in particular, while keeping dose to surrounding normal tissues, rectum and small bowel, at a minimum. Advances in radiotherapy technology have made it possible to more accurately irradiate smaller volumes of tumour with higher doses. Conformal radiotherapy uses multiple collimators to shape the radiation beam much more closely to the contours of the tumour volume while reducing the dose to the surrounding area [47]. Intensity modulated radiotherapy (IMRT) is a more recent form of conformal radiotherapy in which the quantity of radiation across the beam in varied, enabling greater control of the shape of the radiation beam. The radiation beam can be varied to allow higher doses to different areas within the tumour volume [47]. It is important that the CT performed for radiotherapy planning is performed with the same technique and conditions to that later used to administer treatment. Differences in equipment, respiration, oral contrast administered and degree of bladder filling can result in variations in tumour position and volume of tissue within the radiation field. The prostate gland can alter in position within the bony pelvis by 9 mm or more between radiotherapy fractions due to changes in bladder filling [48, 49]. Image guided radiotherapy (IGRT) allows the radiation beam to be altered depending upon day-to-day movement of the prostate gland. This is done by placing intraprostatic fiducial markers (e.g. gold seeds) that serve as surrogates for prostate position, and this in conjunction with IGRT has enhanced the ability to target the prostate despite daily variations with increased accuracy. These techniques are currently being used in the treatment of pelvic malignancy including prostate and bladder carcinomas and require accurate localisation of the tumour margin in order to map out the specific treatment area. CT is principally used although techniques are being developed using MRI image fusion with radiotherapy planning CT for accurate tumour volume co-location.

Magnetic Resonance Imaging

Basic Principles

Magnetic Resonance Imaging (MRI) is a non-ionising radiation method utilising magnetic fields and radiofrequency waves to induce and detect a signal from different body tissues which is then converted into a grey scale image. An MRI scanner consists of a large bore circular magnet. When a patient is placed within it, spinning (precessing) hydrogen ions (protons) in water and lipid molecules of the body tissues are aligned producing a net longitudinal magnetisation along the line of the magnet field. A radiofrequency (RF) pulse at a specific frequency is applied which induces a proportion of precessing, aligned protons to change alignment and flip through an angle, the size of which is determined by the strength and duration of the RF pulse. The net magnetisation is hence tipped into a direction in the transverse plane and induces a small voltage or signal, which can be detected by a receiver coil placed around the patient. When the RF pulse is switched off, the net magnetization begins to decay generating a signal. This signal is amplified and processed into the pixel grey scale level of the MRI image. The strength of the signal partly depends on the proton density of the tissue but more significantly on the time for the transverse magnetisation to decay and the longitudinal magnetisation to re-grow. This is dependent on two methods of energy loss, or relaxation. The T1 relaxation represents recovery of the longitudinal magnetization and depends on the time taken for the excited protons to give up energy and realign themselves along the line of the magnetic field. T1 relaxation is increased by the rapid jostling of heavy molecules within tissues removing energy from the excited protons. Tissues with protons attached to heavy molecules such as proteins or fat have a shorter T1 relaxation time than lightweight molecules containing a high proportion of free water.

T2 relaxation represents decay of the transverse magnetisation and relies on progressive dephasing of excited protons once the RF pulse is switched off. This depends on the variation of local magnetic fields in different tissues which is greatest in solids and rigid large molecules which have a very short T2 compared with free water. Rigid or fixed macromolecules such as those in bone, calculi and metallic clips are relatively immobile and do not generate a signal. By varying time between RF pulses and time to collect the signal, images are produced when the difference of the signal produced by different tissues is greatest. Images are generated with either more T1 or T2 effects or weighting.

Advantages and Disadvantages of MRI Over CT

Compared with CT, MRI produces images which reflect molecular differences between tissues rather than just tissue density and therefore generates a much greater grey scale range of soft tissue contrast. Images can also be generated in any

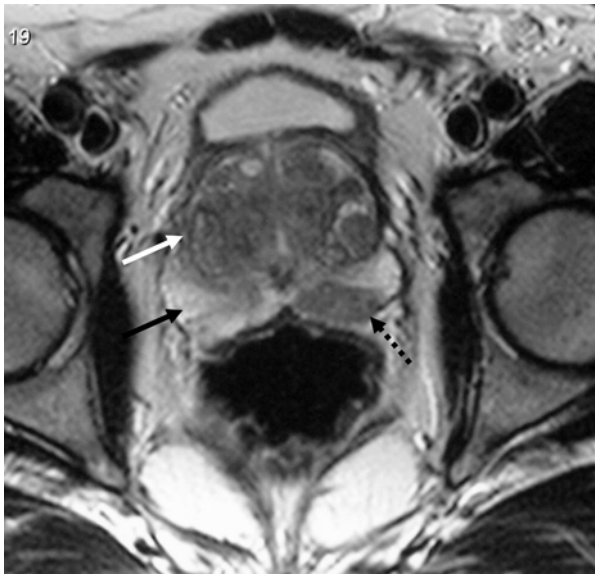

Fig. 5.27 T2 weighted MRI prostate. Axial T2 weighted high resolution image of the mid prostate gland. The normal peripheral zone has a homogenous, high T2 signal intensity (*black arrow*) whilst the central gland has lower T2 signal intensity with nodular changes proportional to the degree of benign prostatic hyperplasia (*white arrow*). Within the left peripheral zone, a typical low signal intensity carcinoma is demonstrated (*dashed arrow*)

plane and at any angle. MRI is particularly useful for imaging the pelvis where contrast and spatial resolution of organs is generally limited with CT. With MRI, molecular differences in the zonal architecture of the prostate can be delineated, for example, and clear distinction between the central and peripheral zones of the gland can be demonstrated (Fig. 5.27). The development of local pelvic RF transmit/receiver coils have enabled imaging to be targeted at a much smaller field of view resulting in improved signal to noise ratio and spatial resolution. This has greatly facilitated the use of MRI in the staging of pelvic malignancy.

Intra-cavity receiver coils have also been developed which are placed into the rectum and produce images with much greater signal-noise ratio. The imaged field of view is much smaller with an endorectal coil but greater resolution can be achieved in the areas imaged. These coils are used particularly to visualize the anal sphincter, prostate zonal anatomy and for rectal cancer staging.

At clinical strengths, MRI does not use ionising radiation and at present poses no known risks to patients. This makes MRI of value where it is desirable to limit radiation exposure, in particular in children or young adults, and patients who require long term follow up surveillance imaging.

MR imaging involves obtaining multiple sequences and planes which is much more time consuming than CT. The imaging sequences obtained are specific to the organ and specialist training of the radiographers and radiologists is essential. Image quality will be degraded by patient movement and respiration and is therefore more dependent on patient cooperation and studies may be limited in sick patients or those requiring continuous monitoring. Some patients are unable to tolerate MRI and find the enclosed confines of the scanner claustrophobic. This may be overcome by using an open bore magnet which is available in some specialist centres.

Technique and Patient Preparation

The patient should be informed that the scan may take up to 30–45min to perform, during which time they will be required to lie still within the scanner. During the scan, loud 'knocking' noises will be heard as radiofrequency pulses are switched on and off. Pelvic MRI for bladder and prostate imaging is best performed with a moderately full bladder, although over distension can result in patient movement artefact. Ideally the patient is asked to void approximately 2 h before the scan. Bowel peristalsis can also create movement artefact and degrade the images. For renal and adrenal MRI an antispasmodic agent such as, buscopan or glucagons is administered immediately prior to the scan [50].

The diagnostic ability of MRI has been enhanced with the now standard use of Gadolinium chelate based intravenous contrast agents. Like iodinated contrast medium used in CT, injected gadolinium circulates within the vascular system and is taken up in vascularised tissue and tumours. Within the magnetic field of the MRI scanner, gadolinium has a paramagnetic effect, causing shortening of the T1 and T2 relaxation times. This is best appreciated on sequences weighted for T1 effects where the signal is increased. Thus, on T1 weighted imaging, vascularized tissue increases in signal intensity following gadolinium administration. Unlike iodinated contrast agents, the incidence of allergic reactions is extremely rare.

Safety Considerations

Ferromagnetic objects placed in or near the magnetic field are attracted to the magnet and can move. This may convert unfixed external objects into potentially hazardous projectiles. Objects within the body such as aneurysm or other surgical clips might be displaced or rotated in body tissues. The current practice is to use MRI-compatible non-magnetic surgical objects where possible. It is important for the MR operator to check the compatibility of surgically inserted materials, particularly those inserted more recently. Joint prostheses are firmly fixed and don't generally cause a problem, although the susceptibility artefact induced by metallic hip prostheses may degrade images of the pelvis. MRI is contraindicated in patients with implantable cardiac pacemakers, neurostimulator devices, cochlear implants, certain types of aneurysm clips and intraocular metallic foreign bodies.

Patients with chronic kidney disease (Stage 4–5) with a GFR of <30 ml/min, those with renal impairment who have had or awaiting liver transplants, those undergoing haemodialysis or peritoneal dialysis, when exposed to gadolinium based contrast agents are at high risk of developing a debilitating fibrosing systemic disease called Nephrogenic systemic fibrosis (NSF). This is thought to be caused by the prolonged presence of gadolinium in the vascular space due to impaired renal clearance. The gadolinium leaks into the extracellular space setting up an irreversible inflammatory reaction. The disease primarily causes patchy fibrosis of the skin and joints, but may also affect the heart, lungs, liver, nerves, dura mater and muscle and may result in increased mortality [51–54]. The risk of NSF is lower for patients with stage 3 chronic kidney disease (GFR 30–59 ml/min) and children under 1 year

due to their immature renal function. It is therefore essential to check patients' serum creatinine and estimated GFR (eGFR levels) before undergoing MRI examination. No cases of NSF have been reported in patients with GFR >60 ml/min [54].

MRI in Urologic Cancers

The main indications for the use of MRI in urologic oncology are summarized in Table 5.5. Because of resource and time implications MRI is often reserved for specific problem-solving such as the characterization of lesions detected by other imaging modalities. This is particularly the case for those renal and adrenal lesions which remain indeterminate on CT, or in whom CT is contraindicated. MRI may also be performed to exclude hepatic metastases in a patient with an indeterminate liver lesion who is being considered for surgery.

Table 5.5 Role of MRI in urologic malignancy

A. Kidney
1. Characterization of focal renal lesions
2. Tumour staging Patients where CT is contraindicated Specific problem solving (a) perinephric invasion (b) local organ invasion (c) venous invasion including IVC wall invasion
3. Follow up/ surveillance: to reduce radiation burden in high risk groups e.g.: VHL
B. Adrenal
1. Characterisation of adrenal mass lesion: Adenoma versus metastasis/ primary adrenal adenocarcinoma
2. Characterisation of functional adrenal mass: Adenoma *versus* adrenal adenocarcinoma
3. Local staging of primary adrenal carcinoma
C. Bladder
1. Local staging
2. Identification of suspected vaginovesical, rectovesical or other fistulae
3. Radiotherapy planning
D. Prostate
1. Local staging Extracapsular invasion Seminal vesicle invasion Nodal staging Multiparametric MRI for tumour detection and localisation
2. Spine MRI: suspected cord compression in patients with bone metastases
E. Testes
No role in assessment of local tumour
Brain and spine MRI for detection of metastases

The exception is for local staging of prostate and bladder carcinoma. MRI is recommended for local staging of muscle invasive bladder cancer and prostate carcinoma in patients being considered for radical treatment. MRI is sensitive for the detection of pelvic fistulae which may arise as a complication of a pelvic tumour, surgery or radiotherapy, and MRI is the imaging investigation of choice for this.

Lesion Characterization

Renal Lesions

Solid renal mass lesions are frequently isointense to renal parenchyma on T1 and hyperintense T2 weighted MRI. Following the administration of Gadolinium they enhance more than renal parenchyma and become more conspicuous [55]. This is particularly important for the detection of small (<3 cm) renal cell carcinomas which are usually solid. MRI is useful for surveillance imaging in high risk patients. In particular, patients with Von Hippel Lindau syndrome, for example, have a propensity to develop renal cell carcinomas, often from a relatively young age and on a background of multiple renal cysts (Fig. 5.28). They frequently develop small (<3 cm) early renal cell carcinomas which are slow growing. MRI is often the imaging method of choice for follow up in these patients.

Adrenal Lesions

MRI techniques have been developed to aid characterization of adrenal lesions. Differentiation of benign from malignant lesions relies on the detection of intracellular lipid, seen almost exclusively within adenomas [28]. This can be reliably detected on MRI with the use of a chemical shift imaging technique. This exploits the normal difference in precessional frequency between fat and water protons

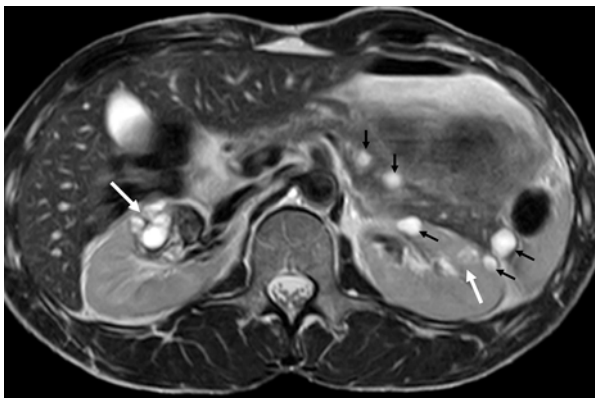

Fig. 5.28 Renal MRI in VHL. Axial T2 weighted MRI image from a male 22 year old patient with Von Hippel Lindau (VHL) syndrome. There are bilateral cystic renal cell carcinomas (*white arrows*) seen as complex cystic masses. Multiple simple cysts are also present within both kidneys and the pancreas (*black arrows*) commonly present in VHL syndrome

Fig. 5.29 Adrenal cortical carcinoma. Coronal T1 weighted post gadolinium MRI in a 26 year old male patient. A large heterogenous right supra-renal mass is demonstrated (*black arrows*). A clear plane of separation is present between the upper pole of the kidney and the mass, congruous with an adrenal mass. The mass shows invasion of the inferior margin of the liver (*white arrows*). Histology confirmed an adrenal cortical carcinoma with direct hepatic invasion

within a given voxel. The protons can be made to precess, or spin, at the same frequency and are 'in phase' with each other and an additive signal is produced. When they are made to precess out of phase the signal is reduced in those voxels which contain both fat and water protons. In the case of adrenal adenomas, the lesion looses signal on the out of phase images compared with the in phase (Fig. 5.18). Adenomas can be diagnosed with up to 100 % specificity [56] and thus can be distinguished from metastases and primary adrenal carcinoma. Primary adrenocortical carcinomas are usually large at presentation, heterogeneous and enhance post Gadolinium administration (Fig. 5.29).

Tumour Staging

Bladder

MRI has the advantage over CT for staging of muscle invasive bladder carcinoma in that it can identify invasion of the deep muscle [50]. It cannot however, differentiate superficial muscle invasion from submucosal invasion. The bladder wall muscle is seen as low signal intensity on T2 weighted images and disruption of this line indicates muscle invasion (Fig. 5.30). MRI is unable to distinguish between T1 and T2 tumours and is inaccurate in assessing T2a versus T2b disease. Its strength is in the demonstration of T3 disease. MRI has better sensitivity for the detection of perivesical fat and surrounding organ invasion, compared with CT. Both T1 and T2 weighted sequences demonstrate T3b disease due to the high signal contrast between tumour and the pelvic fat. MRI is also superior to CT in detecting local organ invasion due

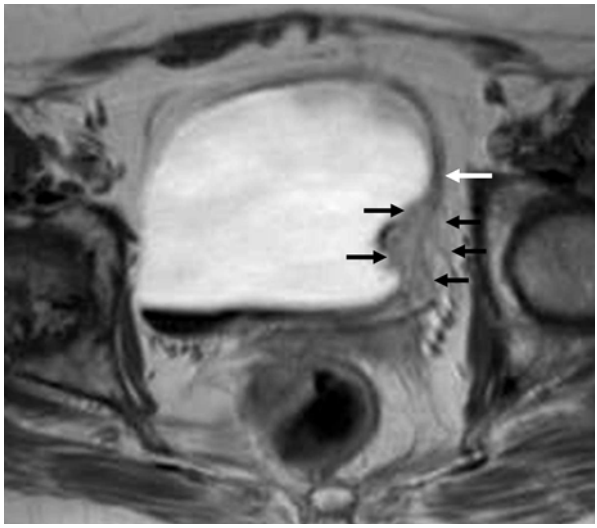

Fig. 5.30 MRI of bladder TCC: T3b carcinoma. Axial T2 weighted image of the bladder with a muscle invasive transitional cell carcinoma along the left lateral bladder wall (*black arrows*). The mass invades the full thickness of the bladder wall which has a low T2 signal intensity (*white arrows*). Tumour is also seen directly invading into the peri-vesical fat in keeping with stage T3b carcinoma

to its superior contrast resolution. The overall accuracy of MRI in staging bladder cancer is 75–85 % and is therefore the modality of choice for local staging of muscle invasive bladder cancer [50].

Patients with pathological T2 stage disease on MRI, are at risk of lymphatic and haematogenous extension and full N and M stage requires CT of the lungs and liver.

Prostate

High resolution T2 weighted imaging of the prostate gland in multiple planes enables the zonal anatomy of the prostate gland to be well demonstrated [57, 58]. The peripheral zone is usually thinner and of higher signal intensity compared with the heterogeneous, lower signal intensity central zone. Prostate carcinoma can be identified as low signal intensity within the peripheral zone (Fig. 5.27). However, this appearance is not specific and can also be seen with chronic inflammation and fibrosis, making detection and delineation of the tumour difficult (Fig. 5.31). Low signal change can also be seen in the peripheral zone due to post biopsy haemorrhage and is confirmed on T1 weighted imaging as high signal foci . The presence of haemorrhage makes it difficult to localize the tumour and reduces staging accuracy when MRI is performed less than 3 weeks post biopsy [59]. Tumours arising within the central zone cannot be differentiated from the markedly heterogeneous appearance of the central zone in co-existent benign prostatic hypertrophy. Tumour localization by MRI is reserved for patients with elevated PSA but previous negative biopsy, and in selected patients MRI has been shown to have a sensitivity and positive predictive value of 83 and 50 % respectively [60].

The principle role of MRI of the prostate, however, is in local tumour staging in patients with histologically proven carcinoma who are being considered for radical

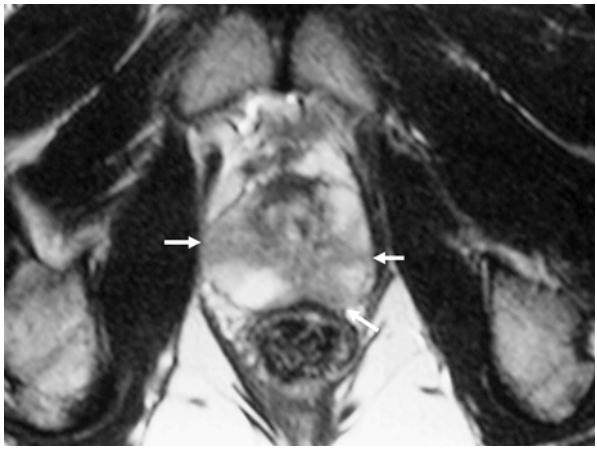

Fig. 5.31 MRI prostate: Non specific prostatitis. Axial T2 weighted image showing multiple bilateral areas of low T2 signal intensity within the peripheral zone of the prostate gland (*white arrows*). Extended biopsies of the prostate gland demonstrated prostatitis only with no foci of carcinoma

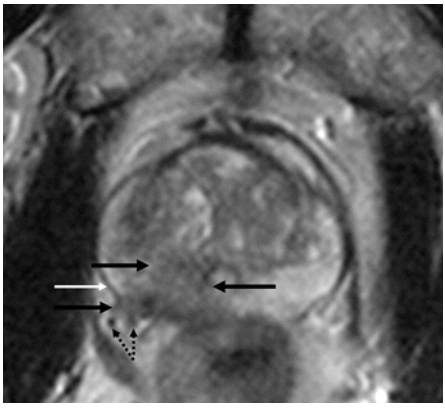

Fig. 5.32 Extracapsular invasion of the prostatic capsule. Axial T2 weighted image of the prostate demonstrating a large focus of carcinoma in the midline and right peripheral zone (*black arrows*). The prostate capsule is well seen (*white arrow*). The tumour in the peripheral zone invades the capsule and extends into the peri-prostatic fat encasing the right neuro-vascular bundle (*dashed arrows*)

surgery or radiotherapy. The accuracy of prostate cancer staging varies but may be up to 88 % with endorectal coil MRI [61]. The detection of extrascapsular extension and seminal vesicle invasion is of particular importance for treatment planning because of their prognostic implications. Features suggesting extracapsular invasion include interruption of the low signal peripheral capsule with a bulging tumour contour but the most predictive features of invasion are asymmetry of the neurovascular bundles and obliteration of the rectoprostatic angle, with specificity of up to 95 % but poor sensitivity of 38 % [62]. The location of the neurovascular bundles are an important site of invasion and can be seen posterolaterally in the 5 and 7 o'clock positions. Loss of the normal rectoprostatic angle at this point is suspicious for tumour extension (Fig. 5.32). Seminal vesicle invasion is suggested when replacement of their normal high signal intensity with low signal intensity tumour is seen (Fig. 5.33). Previous pelvic irradiation, age related atrophy and other benign conditions (e.g.: amyloid) may render the seminal vesicles fibrotic and of low signal intensity. MRI is also important in detection of local tumour invasion into the bladder or rectum.

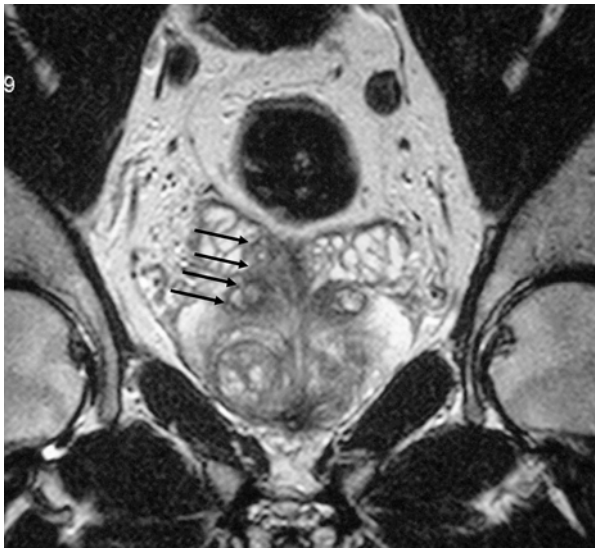

Fig. 5.33 Seminal vesical invasion: T3b carcinoma of the prostate. Coronal T2 weighted image with a tumour focus in the right prostate base, invading the medial aspect of the right seminal vesical. The normal high T2 signal intensity of the seminal vesical is replaced by the low T2 signal intensity of the tumour (*black arrows*)

Multiparametric MRI (MPMri)

Conventional MRI sequences using T1 and T2 weighted images have several limitations in evaluating prostatic disease. It cannot distinguish between tumour, protatitis, haemorrhage and treatment effects. Some tumours are iso-intense to the normal peripheral zone on T2W imaging and central gland tumours are indistinguishable from the normal heterogeneous central gland. After hormonal and radical radiotherapy treatment, the whole prostate gland loses normal zonal anatomy and the peripheral gland loses normal MR signal.

The role of MRI in prostate cancer is evolving with proposed indications which include detecting prostate cancer, localising cancer in the prostate for localised therapies such as HIFU, predicting the aggressiveness of the tumour, detecting recurrence within the prostate following radical radiotherapy and predicting treatment response. For these extended applications, MPMri, in addition to conventional MRI, has been proposed. This includes the use of diffusion weighted imaging (DWI), dynamic contrast enhancement (DCE) and MR spectroscpopy (MRS).

Diffusion weighted imaging MRI technique relies on Brownian motion of molecules and capillary perfusion. It uses balanced positive and negative MR gradients to diphase and then subsequently rephase water protons before signal detection. When no restriction of Brownian motion of water protons occurs, protons move away and no MR signal is acquired . In areas of restricted water motion, rephasing occurs and there is signal acquisition. Restriction of protons occurs in areas of high cellular density or in the presence of extracellular macromolecules. Hence on DW images, areas of restricted diffusion, usually tumours, appear of higher signal intensity. In clinical practice, diffusion can be quantified as ‘apparent’ diffusion coefficient (ADC) value. This is an ‘apparent’ value as the true coefficient is dependent on

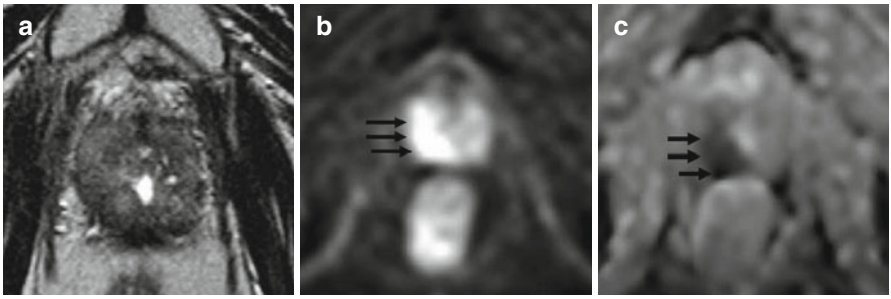

Fig. 5.34 Local recurrence following radical radiotherapy. (**a**) Axial T2 weighted image in a patient following radical radiotherapy treatment. The prostate has a diffuse intermediate T2 signal intensity with complete loss of zonal anatomy. A small localized recurrence within the prostate would be masked by the intermediate signal. (**b**) Axial diffusion weighted image b = 800. The diffusion weighed image demonstrates differential restriction of diffusion within the prostate (*black arrows*). This restricted diffusion is highly suggestive of recurrent disease in the prostate. (**c**) Axial ADC map of the prostate. The ADC image maps the areas of restricted diffusion. A guided biopsy of the sites of restriction (*black arrows*) confirmed recurrent disease in the prostate

temperature, perfusion, motion etc. When used as an adjunct to conventional T2 weighted images, in detection and localization of primary prostate cancer, DWI improves the sensitivity (81 % versus 54 %) compared to T2W sequences alone. There is only a minimal loss of specificity with DWI, 84 % compared to 91 % on T2 weighted images [63, 64]. These results apply to lesions greater than 4 mm in size and Gleeson grade >6. This improvement of tumour detection within the prostate has an important application in guiding TRUS biopsies, detection of local recurrence following radical radiotherapy for salvage local therapies (Fig. 5.34).

During the last decade, dynamic contrast-enhanced MRI has emerged as one of the main techniques used in MPMri of the prostate gland. Dynamic contrast enhanced MRI developed from earlier simpler studies which demonstrated prostate cancer enhanced and washed out earlier than benign prostatic peripheral zone tissue. Fast T1 sequences allow evaluation of contrast dynamics in the prostate following a rapid injection of a gadolinium bolus, reflecting prostate microvascularity and angiogenesis. A rapid continuous series of images obtained (1–7 min) through the whole prostate allows a continuous time assessment of the contrast dynamics in the prostate. These are used to generate an enhancement curves followed by quantitative or semi-quantitative evaluation of the contrast wash-in and wash-out rates. Prostate cancer has higher magnitude of enhancement and a higher wash-in and washout rate compared to benign tissue. The rate of enhancement reflects vascular volume and tissue permeability (corresponds to higher tumour grade). The peak enhancement reflects extravascular/extracellular leakage. Relative peak enhancement has been shown to have the best correlation with malignancy in the peripheral zone [65] (Fig. 5.35).

MR spectroscopy is a 3-dimensional technique for plotting relative concentrations of chemical compounds within the prostate gland by mapping signal intensities of chemicals resonating at different frequencies [66]. Important prostate

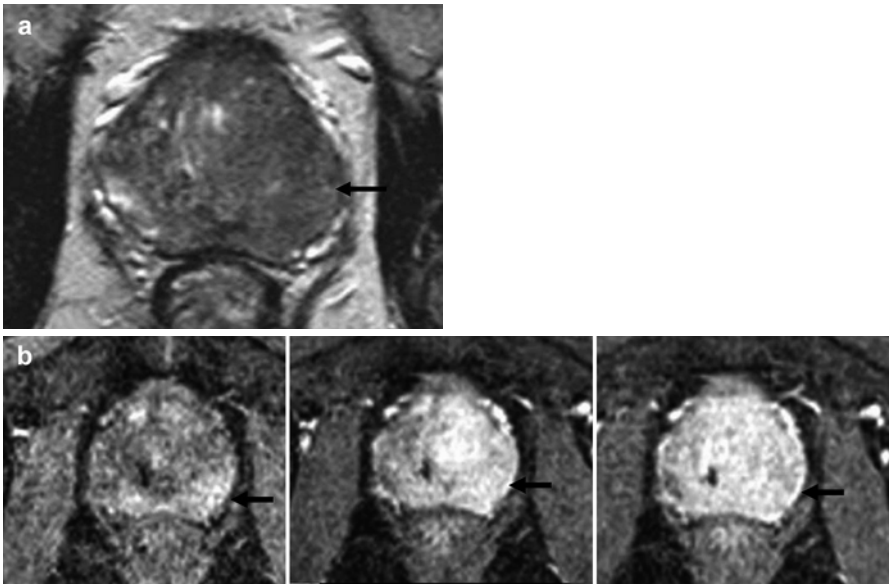

Fig. 5.35 Dynamic contrast enhancement of prostate cancer. (**a**) Axial T2 weighted image in a patient suspected of local recurrent disease (**b**) selected images from the dynamic contrast enhanced sequence at 20, 60 and 120s showing typical early tumoural enhancement in the left sided peripheral zone (*black arrows*)

metabolites are Polyamines, Choline which resonate at 3.25 ppm, Creatine resonates at 3.05 ppm and Citrate resonates at 2.62 ppm. In normal peripheral zone a relatively high peak of citrate is seen compared to that of choline. Choline is a normal constituent of cell membranes and in areas of high tumour cell turnover, a relative increase in the concentration of choline is seen, with reduction of choline. This leads to a reversal of the normal choline: citrate ratio. Spatial mapping of such peaks within the prostate gland are used to plot the location and estimate the extent of tumour (Fig. 5.36). When used in conjunction with standard endorectal or pelvic phased array prostate MR, this technique has been shown to improve tumour localisation [67], increase staging accuracy and reduce interobserver variability. The ability of MRS to identify cancer is dependent on (i) **tumor size**; cancers < 0.5 cm in diameter may be missed whereas those > 0.5 cm are identified with increasing accuracy, (ii) **tumour grade**; higher grades (Gleason score 8–10) are better imaged than lower grade tumours [68].

The increased sensitivity of MPMri in tumour detection and localization provide a useful guide to biopsy of the prostate in patients with rising PSA but previous negative biopsies. The fusion of ultrasound and MPMri software allows the benefits of both techniques to be harnessed in increasing the positive yield of prostatic biopsies. Magnetic resonance imaging/ultrasound fusion guided biopsies can detect more cancers per core than standard 12-core transrectal ultrasound biopsy for all levels of suspicion on magnetic resonance imaging [69].

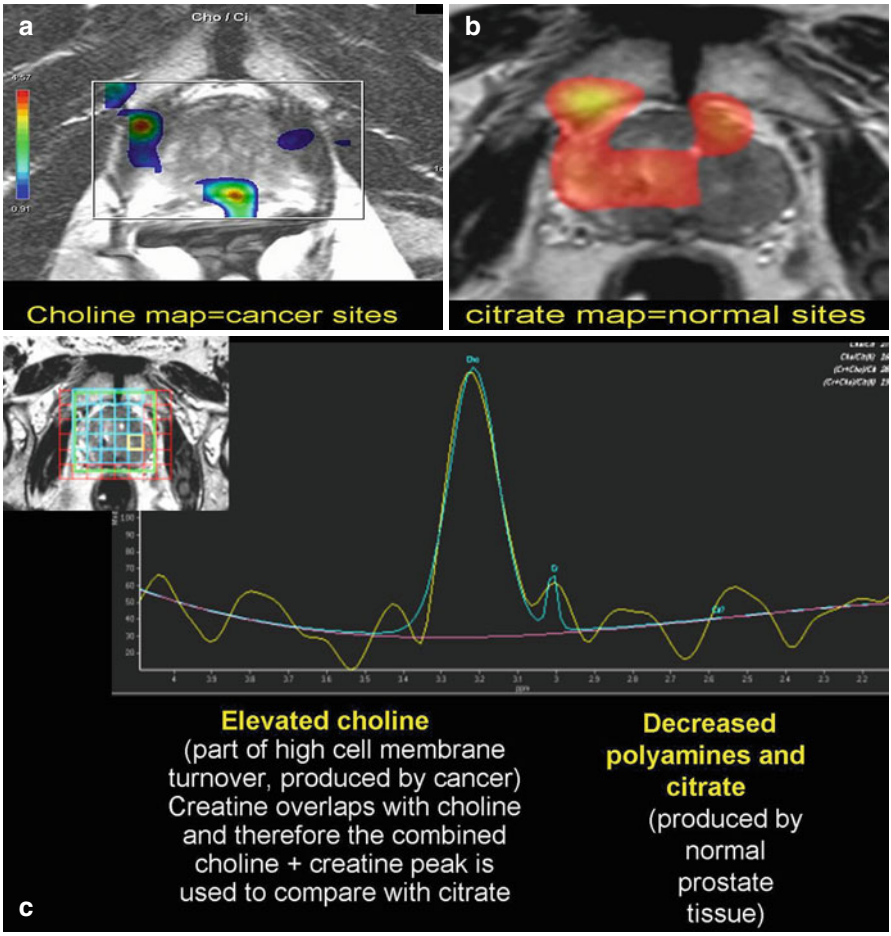

Fig. 5.36 Spectroscopy citrate and choline maps. (**a**) Spectroscopic data acquired through the prostate can be displayed over conventional T2 weighted images. Sites with high levels of choline have been displayed as blue and correspond to tumour sites in both peripheral zones. (**b**) Similarly, citrate maps can also be created, demonstrating areas of normal prostatic tissue. An extensive tumour is seen in the left peripheral zone with no citrate substrate. (**c**) Spectroscopic data can also be displayed as a spectroscopic trace of substrates in each voxel. An elevated choline plus creatine peak and a reduction in the citrate and polyamines corresponds to tumour

Specific Problem-Solving in Renal and Adrenal Carcinoma Staging

In the case of renal and adrenal staging, MRI is usually reserved for resolving specific problems not answered with CT. The multiplanar imaging ability of MRI can help delineate the organ of origin of a large suprarenal or renal angle mass. Similarly, local organ invasion may be better differentiated with MRI where accuracy rates of

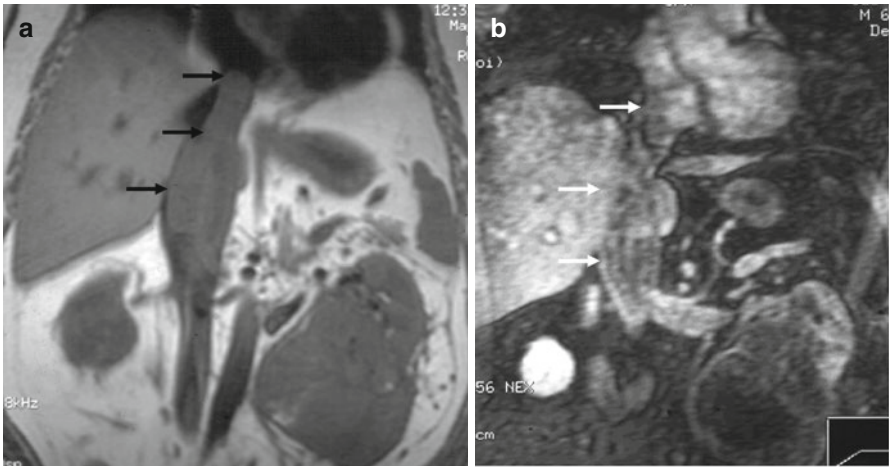

Fig. 5.37 IVC thrombus on MRI. (**a**) Coronal T1 weighted MRI. A large left lower pole carcinoma with expansion of left renal vein and IVC (*arrows*). The upper level of thrombus is well visualized within the supra-diaphragmatic IVC. (**b**) Coronal T1 weighted MRI post gadolinium enhanced image showing non-enhancing thrombus within the IVC (*arrows*)

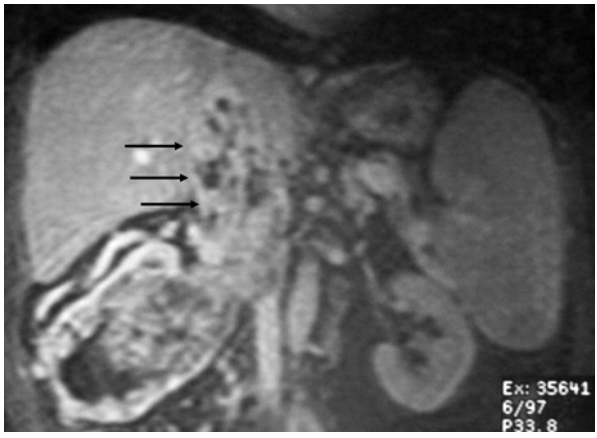

Fig. 5.38 IVC wall invasion on MRI. Coronal T1 weighted image following intravenous gadolinium enhancement. The wall of the IVC is invaded by the enhancing tumour thrombus within the lumen of the IVC (*arrows*). Both the wall and the tumour have heterogenous enhancement and no nomal IVC wall is seen at the site of the luminal tumour. These features are highly specific for IVC wall invasion

up to 100 % have been reported [70] for renal cell carcinoma. The main role of MRI in renal and adrenal staging is in the diagnosis of venous tumour thrombosis, and the delineation the uppermost level of extension. The suprahepatic IVC and right atrium, which may be difficult to visualise on CT, are well seen with MRI (fig. 5.37). Enhancement of thrombus following Gadolinium administration enables distinction between bland and tumour thrombus to be made [71]. Direct tumour thrombus invasion of the caval wall can also be diagnosed with 92 to 94 % accuracy [71, 72] with contrast enhanced MRI (Fig. 5.38). Gadolinium-enhanced 3-dimensional MRI studies can be used to generate renal angiographic images and provide a preoperative vascular roadmap for potentially resectable tumours.

Conclusion

Ultrasound remains an important first line investigation in the detection of renal and testicular cancer, in children and pregnant women. The main imaging modality for uro-oncological cancer staging, treatment planning and surveillance is CT. MRI is used mainly as a problem solving tool for renal and testicular cancer but has the best imaging performance for the local staging of bladder and prostate cancer. Along with the myriad of traditional applications of imaging, advances in multiparametric MRI, multi-detector CT and 3D ultrasound, continue to widen the horizons of cross-sectional imaging. Image guided therapy for renal and prostate cancer are now well established. MRI is being advocated to guide prostate biopsy and stratify treatment options. Advances in MPMri will continue to see increasing applications in the management of patients with prostate cancer.

References

1. Dalla PL. What is left of i.v. urography? Eur Radiol. 2001;11(6):931–9.
2. Chalmers N, Jackson RW. Comparison of iodixanol and iohexol in renal impairment. Br J Radiol. 1999;72(859):701–3.
3. Yousem DM, Gatewood OM, Goldman SM, Marshall FF. Synchronous and metachronous transitional cell carcinoma of the urinary tract: prevalence, incidence, and radiographic detection. Radiology. 1988;167(3):613–8.
4. Kang CH, Yu TJ, Hsieh HH, et al. The development of bladder tumors and contralateral upper urinary tract tumors after primary transitional cell carcinoma of the upper urinary tract. Cancer. 2003;98(8):1620–6.
5. Joffe SA, Servaes S, Okon S, Horowitz M. Multi-detector row CT urography in the evaluation of hematuria. Radiographics. 2003;23(6):1441–55.
6. McNicholas MM, Raptopoulos VD, Schwartz RK, et al. Excretory phase CT urography for opacification of the urinary collecting system. Am J Roentgenol. 1998;170:1261–7.
7. Caoili EM, Cohan RH, Korobkin M, et al. Urinary tract abnormalities: initial experience with multi-detector row CT urography. Radiology. 2002;222(2):353–60.
8. Nawfel RD, Judy PF, Schleipman AR, Silverman SG. Patient radiation dose at CT urography and conventional urography. Radiology. 2004;232:126–32.
9. Portnoy O, Guranda L, Apter S, Eiss D, Amitai MM, Konen E. Optimization of 64-MDCT Urography: Effect of Dual-Phase Imaging With Furosemide on Collecting System Opacification and Radiation Dose. AJR Am J Roentgenol. 2011;197(5):W882–6.
10. Van Der Molen AJ, Cowan NC, Mueller-Lisse UG, Nolte-Ernsting CC, Takahashi S, Cohan RH. CT Urography Working Group of the European Society of Urogenital Radiology (ESUR). CT urography: definition, indications and techniques. A guideline for clinical practice. Eur Radiol. 2008;18(1):4–17.
11. Kawashima A, Glockner JF, King Jr BF. CT urography and MR urography. Radiol Clin North Am. 2003;41(5):945–61.
12. Thompson IM, Peek M. Improvement in survival of patients with renal cell carcinoma- the role of the serendipitously detected tumor. J Urol. 1988;140(3):487–90.
13. Pantuck AJ, Zisman A, Belldegrun AS. The changing natural history of renal cell carcinoma. J Urol. 2001;166(5):1611–23.
14. Habboub HK, Abu-Yousef MM, Williams RD, et al. Accuracy of color Doppler sonography in assessing venous thrombus extension in renal cell carcinoma. Am J Roentgenol. 1997;168(1):267–71.

15. Kallman DA, King BF, Hattery RR, et al. Renal vein and inferior vena cava tumor thrombus in renal cell carcinoma: CT, US, MRI and venacavography. J Comput Assist Tomogr. 1992;16(2):240–7.
16. Robbin ML. Ultrasound contrast agents: a promising future. Radiol Clin North Am. 2001;39:399–414.
17. Jakobsen JA. Ultrasound contrast agents: clinical applications. Eur Radiol. 2001;11(8):1329–37.
18. Jayson M, Sanders H. Increased incidence of serendipitously discovered renal cell carcinoma. Urology. 1998;51(2):203–5.
19. Bosniak MA. The current radiological approach to renal cysts. Radiology. 1986;158:1–10.
20. Bosniak MA. The small (less than or equal to 3.0 cm) renal parenchymal tumor: detection, diagnosis, and controversies. Radiology. 1991;179(2):307–17.
21. Israel GM, Bosniak MA. Follow-up CT of moderately complex cystic lesions of the kidney (Bosniak category IIF). Am J Roentgenol. 2003;181(3):627–33.
22. Abecassis M, McLoughlin MJ, Langer B, Kudlow JE. Serendipitous adrenal masses: prevalence, significance, and management. Am J Surg. 1985;149(6):783–8.
23. Glazer HS, Weyman PJ, Sagel SS, et al. Nonfunctioning adrenal masses: incidental discovery on computed tomography. Am J Roentgenol. 1982;139(1):81–5.
24. Mitnick JS, Bosniak MA, Megibow AJ, Naidich DP. Non-functioning adrenal adenomas discovered incidentally on computed tomography. Radiology. 1983;148:495–9.
25. Francis IR, Smid A, Gross MD, et al. Adrenal masses in oncologic patients: functional and morphologic evaluation. Radiology. 1988;166(2):353–6.
26. Krestin GP, Freidmann G, Fishbach R, et al. Evaluation of adrenal masses in oncologic patients: dynamic contrast-enhanced MR vs CT. J Comput Assist Tomogr. 1991;15(1):104–10.
27. Frilling A, Tecklenborg K, Weber F, et al. Importance of adrenal incidentaloma in patients with a history of malignancy. Surgery. 2004;136(6):1289–96.
28. Korobkin M, Giordano TJ, Brodeur FJ, et al. Adrenal adenomas: relationship between histologic lipid and CT and MR findings. Radiology. 1996;200(3):743–7.
29. Boland GW, Lee MJ, Gazelle GS, et al. Characterization of adrenal masses using unenhanced CT: an analysis of the CT literature. Am J Roentgenol. 1998;171:201–4.
30. Korobkin M, Brodeur FJ, Francis IR, et al. CT time-attenuation washout curves of adrenal adenomas and nonadenomas. Am J Roentgenol. 1998;170(3):747–52.
31. Pena CS, Boland GW, Hahn PF, et al. Characterization of indeterminate (lipid-poor) adrenal masses: use of washout characteristics at contrast-enhanced CT. Radiology. 2000; 217(3):798–802.
32. Francis IR, Casalino DD, Arellano RS, Baumgarten DA, Curry NS, Dighe M, et al. ACR Appropriateness Criteria® incidentally discovered adrenal mass. Reston: American College of Radiology (ACR); 2009.
33. Johnson CD, Dunnick NR, Cohan RH, Illescas FF. Renal adenocarcinoma: CT staging of 100 tumors. Am J Roentgenol. 1987;148(1):59–63.
34. Fein AB, Lee JK, Balfe DM, et al. Diagnosis and staging of renal cell carcinoma: a comparison of MR imaging and CT. Am J Roentgenol. 1987;148(4):749–53.
35. Studer UE, Scherz S, Scheidegger J, et al. Enlargement of regional lymph nodes in renal cell carcinoma is often not due to metastases. J Urol. 1990;144(2 Pt 1):243–5.
36. Catalano C, Fraioli F, Laghi A, et al. High-resolution multidetector CT in the preoperative evaluation of patients with renal cell carcinoma. Am J Roentgenol. 2003;180(5):1271–7.
37. Clayman Jr RV, Gonzalez R, Fraley EE. Renal cancer invading the inferior vena cava: clinical review and anatomical approach. J Urol. 1980;123(2):157–63.
38. Hatcher PA, Anderson EE, Paulson DF, et al. Surgical management and prognosis of renal cell carcinoma invading the vena cava. J Urol. 1991;145(1):20–3.
39. MacVicar D. Staging of testicular germ cell tumours. Clin Radiol. 1993;47:149–58.
40. Dixon AK, Ellis M, Sikora K. Computed tomography of testicular tumours: distribution of abdominal lymphadenopathy. Clin Radiol. 1986;37(6):519–23.
41. Williams MP, Cook JV, Duchesne GM. Psoas nodes-an overlooked site of metastasis from testicular tumours. Clin Radiol. 1989;40(6):607–9.

42. Coll DM, Uzzo RG, Herts BR, et al. 3-dimensional volume rendered computerized tomography for preoperative evaluation and intraoperative treatment of patients undergoing nephron sparing surgery. J Urol. 1999;161(4):1097–102.
43. Smith PA, Marshall FF, Corl FM, Fishman EK. Planning nephron-sparing renal surgery using 3D helical CT angiography. J Comput Assist Tomogr. 1999;23(5):649–54.
44. Coll DM, Herts BR, Davros WJ, Uzzo RG, Novick AC. Preoperative use of 3D volume rendering to demonstrate renal tumors and renal anatomy. Radiographics. 2000;20(2):431–8.
45. Sheth S, Scatarige JC, Horton KM, Corl FM, Fishman EK. Current concepts in the diagnosis and management of renal cell carcinoma: role of multidetector ct and three-dimensional CT. Radiographics 2001;21 Spec No:S237–54.
46. Young ST, Paulson EK, McCann RL, Baker ME. Appearance of oxidized cellulose (Surgicel) on postoperative CT scans: similarity to postoperative abscess. AJR Am J Roentgenol. 1993;160(2):275–7.
47. Mangar SA, Huddart RA, Parker CC, et al. Technological advances in radiotherapy for the treatment of localised prostate cancer. Eur J Cancer. 2005;41(6):908–21.
48. Langen KM, Jones DTL. Organ motion and its management. Int J Radiat Oncol Biol Phys. 2001;50:265–78.
49. Balter JM, Sandler HM, Lam K, Bree RL, Lichter AS, Ten Haken RK. Measurement of prostate movement over the course of routine radiotherapy using implanted markers. Int J Radiat Oncol Biol Phys. 1995;31:113–8.
50. Mallampati GK, Siegelman ES. MR imaging of the bladder. Magn Reson Imaging Clin N Am. 2004;12:545–55.
51. Saenz A, Mandal R, Kradin R, Hedley-Whyte ET. Nephrogenic fibrosing dermopathy with involvement of the dura mater. Virchows Arch. 2006;449:389–91.
52. Mendoza FA, Artlett CM, Sandorfi N, et al. Description of 12 cases of nephrogenic fibrosing dermopathy and review of the literature. Semin Arthritis Rheum. 2006;35:238–49.
53. Perez-Rodriguez J, Lai S, Ehst BD, et al. Nephrogenic systemic fibrosis: incidence, associations, and effect of risk factor assessment – report of 33 cases. Radiology. 2009;250:371–7.
54. Gadolinium based contrast media and Nephrogenic systemic fibrosis. The Royal College of Radiologists, Board of the Faculty of Clinical Radiology. November 2007. http://www.rcr.ac.uk/docs/radiology/pdf/BFCR0714_Gadolinium_NSF_guidanceNov07.pdf. Last accessed on 31 Oct 2013.
55. Rominger MB, Kenney PJ, Morgan DE, et al. Gadolinium-enhanced MR imaging of renal masses. Radiographics. 1992;12(6):1097–116.
56. Korobkin M, Lombardi TJ, Aisen AM, et al. Characterization of adrenal masses with chemical shift and gadolinium-enhanced MR imaging. Radiology. 1995;197(2):411–8.
57. Heiken JP, Forman HP, Brown JJ. Neoplasms of the bladder, prostate, and testis. Radiol Clin North Am. 1994;32(1):81–98.
58. Huch Boni RA, Boner JA, Debatin JF, et al. Optimization of prostate carcinoma staging: comparison of imaging and clinical methods. Clin Radiol. 1995;50(9):593–600.
59. White S, Hricak H, Forstner R, et al. Prostate cancer: effect of postbiopsy hemorrhage on interpretation of MR images. Radiology. 1995;195(2):385–90.
60. Beyersdorff D, Taupitz M, Winkelmann B, et al. Patients with a history of elevated prostate-specific antigen levels and negative transrectal US-guided quadrant or sextant biopsy results: value of MR imaging. Radiology. 2002;224(3):701–6.
61. Yu KK, Hricak H, Alagappan R, et al. Detection of extracapsular extension of prostate carcinoma with endorectal and phased-array coil MR imaging: multivariate feature analysis. Radiology. 1997;202(3):697–702.
62. Yu KK, Scheidler J, Hricak H, et al. Prostate cancer: prediction of extracapsular extension with endorectal MR imaging and three-dimensional proton MR spectroscopic imaging. Radiology. 1999;213(2):481–8.
63. Haider MA, van der Kwast TH, Tanguay J, Evans AJ, Hashmi AT, Lockwood G, Trachtenberg J. Combined T2-weighted and diffusion-weighted MRI for localization of prostate cancer. AJR Am J Roentgenol. 2007;189(2):323–8.

64. desouza NM, Reinsberg SA, Scurr ED, Brewster JM, Payne GS. Magnetic resonance imaging in prostate cancer: the value of apparent diffusion coefficients for identifying malignant nodules. Br J Radiol. 2007;80(950):90–5. Epub 2007 Feb 15.
65. Engelbrecht MR, Huisman HJ, Laheij RJ, Jager GJ, van Leenders GJ, Hulsbergen-Van De Kaa CA, et al. Discrimination of prostate cancer from normal peripheral zone and central gland tissue by using dynamic contrast-enhanced MR imaging. Radiology. 2003;229(1): 248–54. Epub 2003 Aug 27.
66. Claus FG, Hricak H, Hattery RR. Pretreatment evaluation of prostate cancer: role of MR imaging and 1H MR spectroscopy. Radiographics. 2004;24 Suppl 1:S167–80.
67. Rajesh A, Coakley FV. MR imaging and MR spectroscopic imaging of prostate cancer. Magn Reson Imaging Clin N Am. 2004;12(3):557–79.
68. Zakian KL, Sircar K, Hricak H, Chen HN, Shukla-Dave A, Eberhardt S, et al. Correlation of proton MR spectroscopic imaging with gleason score based on step-section pathologic analysis after radical prostatectomy. Radiology. 2005;234(3):804–14.
69. Pinto PA, Chung PH, Rastinehad AR, Baccala Jr AA, Kruecker J, Benjamin CJ, et al. Magnetic resonance imaging/ultrasound fusion guided prostate biopsy improves cancer detection following transrectal ultrasound biopsy and correlates with multiparametric magnetic resonance imaging. J Urol. 2011;186(4):1281–5. Epub 2011 Aug 17.
70. Hricak H, Thoeni RF, Carroll PR, et al. Detection and staging of renal neoplasms: a reassessment of MR imaging. Radiology. 1988;166(3):643–9.
71. Aslam Sohaib SA, Teh J, Nargund VH, et al. Assessment of tumor invasion of the vena caval wall in renal cell carcinoma cases by magnetic resonance imaging. J Urol. 2002;167(3):1271–5.
72. Myneni L, Hricak H, Carroll PR. Magnetic resonance imaging of renal carcinoma with extension into the vena cava: staging accuracy and recent advances. Br J Urol. 1991;68:571–8.